AD-A096 057 AIR FORCE INST OF TECH WRIGHT-PATTERSON AFB OH SCHOO--ETC F/G 20/4
A SINGULAR PERTURBATION METHOD FOR ARBITRARY CONFIGURATIONS IN --ETC(U)
OCT 80 F M JONAS

UNCLASSIFIED AFIT/DS/AA/80-3 NL

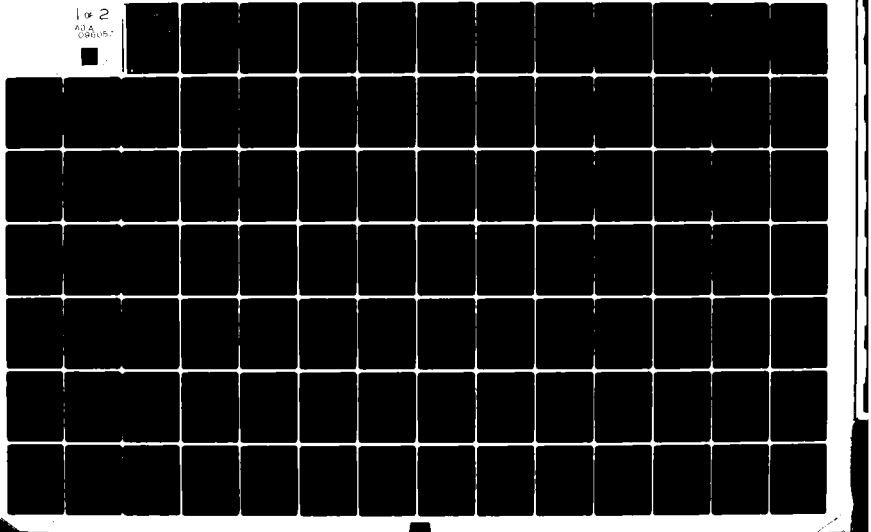

LEVEL II

A SINGULAR PERTURBATION METHOD FOR ARBITRARY CONFIGURATIONS IN SUBSONIC POTENTIAL FLOW

DISSERTATION

AFIT/DS/AA/80-3 Frederick M. Jonas
Capt. USAF

AFIT/DS/AA/80-3

APPROVED FOR PUBLIC RELEASE AFR 190-17. 27 FEB 1981

FREDRIC C. LYNCH, Major, USAF
Director of Public Affairs

Air Force Institute of Technology (ATC)
Wright-Patterson AFB, OH 45433

A SINGULAR PERTURBATION METHOD FOR ARBITRARY CONFIGURATIONS IN SUBSONIC POTENTIAL FLOW.

DISSERTATION

AFIT/DS/AA/80-3 Frederick M. Jonas
Capt USAF

Approved for public release; distribution unlimited

AFIT/DS/AA/80-1

A SINGULAR PERTURBATION METHOD FOR ARBITRARY CONFIGURATIONS IN SUBSONIC POTENTIAL FLOW

DISSERTATION

Presented to the Faculty of the School of Engineering
of the Air Force Institute of Technology
Air University
in Partial Fulfillment of the
Requirements for the Degree of
Doctor of Philosophy

by

Frederick M. Jonas, B.S., M.S.
Capt USAF

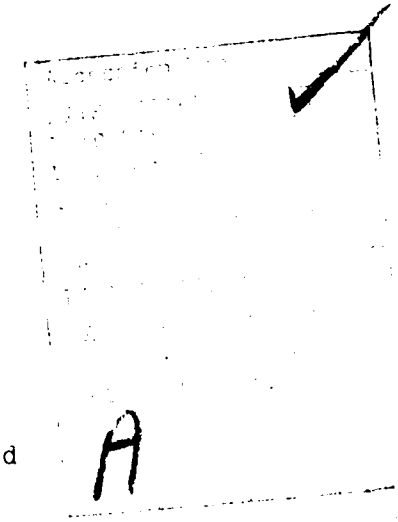

AFIT/DS/AA/80-3

A SINGULAR PERTURBATION METHOD FOR ARBITRARY CONFIGURATIONS IN SUBSONIC POTENTIAL FLOW

by

Frederick M. Jonas, B.S., M.S.
Capt USAF

Approved:

Stephen J. Kovalsky Chairman	23 Oct 80
James J. Olsen	23 Oct 80
Harold E. Wright	24 Oct 80
Dennis W. Quinn	17 Nov 80
David Allan Lee	18 Nov 80

Accepted:

Edward J. Kozniewski Dean, School of Engineering	18 Nov 80

Acknowledgements

"The things which impossible with men are possible with God." (Luke 19:27)

This effort is dedicated to my wife Jan, and my sons Freddy and Daniel, without whose love and understanding nothing would have been accomplished. My thanks to my Advisory Committee chairman, Major Stephen J. Koob, committee members Professors David A. Lee, Harold E. Wright, Dennis Quinn, and former members Frank E. Eastep and John Shea, for their patient guidance and advice. Finally, a special thanks to Dr. Rimantas Liaugminas, ASD/ENFTA, for his help in the use of and providing the Woodward and Jameson codes, and to Dr. Tom Weeks, AFWAL/FIMM, for sponsoring this effort.

Contents

Contents

List of Figures

List of Figures

List of Tables

List of Symbols

Symbol	Definition
a	speed of sound (ft/sec)
c	composite solution (subscript/superscript), or chord length (ft)
C_D	drag coefficient, $D/\frac{1}{2}\rho_\infty U_\infty^2 S$
C_d	section (2-D) drag coefficient, $D'/\frac{1}{2}\rho_\infty U_\infty^2 c$
C_p	pressure coefficient, $p-p_\infty/\frac{1}{2}\rho_\infty U_\infty^2$
D	drag (lb_f)
D'	section drag (lb_f/ft)
$F(x,y,z)$	surface equation, $F(x,y,z)=0$ on the surface
$f(\zeta)$	complex potential function (2-D)
i	inner solution (subscript/superscript), or imaginary number, $\sqrt{-1}$
I	intermediate solution (subscript/superscript)
ℓ	characteristic length (ft)
M	Mach number, V/a
n	outward surface normal vector
o	outer solution (subscript/superscript)
S	reference area (ft^2)
U	velocity (ft/sec)
(u,v,w)	perturbation velocity components (ft/sec) in Cartesian coordinate system
V	velocity (ft/sec)
(x,y,z)	Cartesian coordinates
Y	complex variable, $x+iz$
β	$\sqrt{1-M_\infty^2}$
γ	ratio of specific heats, or complex variable
ϵ	perturbation parameter

List of Symbols

Symbol	Definition
f	complex variable, $\xi + i\eta$
θ	body meridan angle (deg)
(μ, ν)	elliptic coordinates
(ξ, η)	Cartesian coordinates
ρ	density (slug/ft)
φ	perturbation potential function
Φ	total potential function
χ	stream function
∞	free stream conditions (subscript)
$\binom{n}{m}$	binomial coefficient, n!/(n-m)!m!

Abstract

A method is developed for obtaining uniformly valid solutions about slender bodies (2-D or 3-D) with round leading/trailing edges in compressible subsonic flow. The method is based on the principles of singular perturbation theory and applied to nonlifting thickness problems. The method corrects small perturbation theory (outer solution) with a stagnation region theory (inner solution) yielding uniformly valid solutions. Analytic results of the first and second order method are presented and compared to other methods, including exact numerical results, for the elliptic cylinder. The first order method is shown to be preferred to higher order efforts and is directly applicable to current numerical techniques solving the Prandtl-Glauert equation. Application of the first order method numerically, using a current panel technique, is presented for the NACA 0012 airfoil and a glide bomb configuration. All comparisons of the first order composite results with other methods show excellent agreement and improved results subject to the limits of validity of the theory. The ability to correctly model the flow behavior in stagnation regions using the composite solutions leads to a greater confidence in aerodynamic predictions, especially inviscid drag estimates.

1 Introduction

The purpose of this dissertation is to develop a method, based on the principles of singular perturbation theory, for obtaining uniformly valid solutions for flow about slender bodies with round leading or trailing edges in subsonic potential flow. Specifically the method improves solutions obtained from the linearized small perturbation potential equation (Prandtl-Glauert equation) in stagnation regions. The ability to correctly model the behavior in stagnation regions leads to a greater confidence in aerodynamic predictions, especially inviscid drag estimates. The first order method is shown to be preferable to a second order effort, and is directly applicable to current numerical techniques solving the Prandtl-Glauert equation. Results of the first order method are compared to numerical solutions of the exact potential equation, and are shown to be in excellent agreement subject to the limits of validity of the theory. The present development is for nonlifting bodies only.

Background

In recent years there has been considerable theoretical and engineering development of numerical techniques for the prediction of potential flow about arbitrary configurations. For compressible flows the most useful methods to date for arbitrary configurations (2-D or 3-D) have been the surface singularity methods, or panel methods (Ref 1-6). The solutions obtained by these methods for steady compressible flow

are solutions to the well known Prandtl-Glauert equation. This equation is derived from the exact potential equation based on the assumption of small perturbations or disturbances, and is valid for subsonic or supersonic flow (Ref 7). Solutions thus obtained offer reasonable predictions of inviscid lift and pitching moment, and surface pressure distributions except in stagnation regions (Ref 8,9). The failure of these methods in stagnation regions often results in the prediction of unrealistically high surface velocities, and thus poor surface pressure estimates in these regions. The overall result is poor inviscid drag estimates, especially for configurations with round or blunt edges, where the local slopes are greatest (drag being the integral of pressure times slope in the free stream direction). This failure is directly related to the fact that the assumption of small perturbations in the stagnation region is very poor.

History of Previous Efforts

Thin airfoil and slender body theory provided aerodynamicists the first opportunities to make accurate estimates of the potential flowfield about arbitrary configurations, especially for those immersed in a compressible flow. It was recognized by many investigators however, that these results were not accurate in stagnation regions. A method to correct thin airfoil theory in stagnation regions was developed by Lighthill (Ref 10), while an alternate approach obtaining the same results was developed by Van Dyke (Ref 11). These methods are typified by Riegel's rule (Ref 11). With the advent

of electronic computers, and the more exact modeling obtainable with surface singularity methods, the above mentioned methods are rarely used. Current emphasis seems to be directed at correcting the resultant inviscid drag estimates based on the theoretical results of Jones (Ref 12,13) as presented by Sotomayer and Weeks (Ref 14). This approach involves estimating the amount of leading edge suction, and thus leading edge thrust or drag, necessary to obtain accurate results. A much different and fortuitous approach developed by Stancil (Ref 8) for improving supersonic wave drag estimates could also be used for subsonic applications. This method, deemed modified linear theory, solves the Prandtl-Glauert equation based on the local Mach number instead of the free stream Mach number. Each of these methods will now be discussed in more detail, with acknowledgements to each for providing insights into the present method.

As mentioned, the methods developed by Lighthill and Van Dyke are for correcting the results obtained from thin airfoil theory in stagnation regions. Since Lighthill's method is valid only for round edges, and his results are duplicated by Van Dyke, only the method as presented by Van Dyke will be discussed. Van Dyke's method is based on the principles of singular perturbation theory and the theory of matched asymptotic expansions. Two regions in the flowfield about a slender body are clearly identified, the dominant region being one of small disturbances from the free stream conditions and the other being the stagnation region. The results

of thin airfoil theory are salvaged (Ref 11) by applying a multiplicative corredtion which is dependent on the shape of the surface in the stagnation region. For round edges in incompressible 2-D flows, the flowfield in the stagnation region is approximated by the exact incompressible flow about a parabola, chosen to match as closely as possible the given geometry in the stagnation region. This forms the basis for the correction. For round edges in compressible flows, the exact solution for the flow about a parabola is not known and must be approximated using a Janzen-Rayleigh expansion or experimental data. The thin airfoil results themself are of course extended to compressible flow using the Prandtl-Glauert compressibility correction. This method for sharp edges follows the same approach using the flow about a wedge to form the basis for the correction. The region of non-uniformity for sharp edges in compressible flow is so small that any correction is negligible and therefore not used. Thus the method just described is applicable only to the results obtained from thin airfoil theory (2-D), and exact only for incompressible flow. Extensions to the more exact modeling available using surface singularity methods, and to 3-D configurations, has not been adequately developed.

The method developed by Sotomayer and Weeks to improve inviscid drag estimates obtained using panel methods is representative of methods based on the theoretical results of Jones. Jones showed that when applying thin airfoil theory to an airfoil with a rounded nose in incompressible flow,

the resultant pressure distribution in the stagnation region is in error. In evaluating the drag using these results one must add a leading edge drag term to obtain the correct inviscid 2-D result, that being zero. (Note that for the lifting problem, or flat plate at angle of attack, one must add a leading edge thrust term.) The error is due to a leading edge singularity which is an essential part of the thin airfoil theory solution. The method of Sotomayer and Weeks attempts to extend the correction (leading edge thrust/drag) developed by Jones for 2-D incompressible flow to 3-D wings, correcting for compressibility and sweep. For 2-D flows the amount of leading edge thrust/drag required is easily determined since one knows beforehand the desired result (zero), but for 3-D flows (induced drag) this is not the case and one requires some other criteria to base the correction on. Normally other empirical or experimental data for similar configurations is used as this basis for determining the level of the correction required. Thus while this technique can produce favorable results in comparison with test data, the difficulty arises in predicting the amount of correction necessary. Although there are guidelines, the amount of leading edge thrust necessary can vary from zero (no correction) to 100% of the theoretical value, and is by no means analytically determined.

Stancil's modified linear theory was developed to improve supersonic wave drag calculations, but could also be applied to subsonic flows. The foundation of the method is

is the Prandtl-Glauert equation based on local Mach number instead of the free stream Mach number:

$$(1 - M^2)\varphi_{xx} + \varphi_{yy} + \varphi_{zz} = 0 \qquad (1)$$

On examining this equation it is evident that as the local Mach number (or velocity) approaches zero in the stagnation region, Laplace's equation results. On the other hand for flow over a slender body, where the local Mach number is approximately the free stream value, the Prandtl-Glauert equation results. (This again points out the diverse nature of the various flowfield regions.) The method is applied using current panel techniques with surface singularity distributions. The exact surface velocity boundary condition (as opposed to thin airfoil type approximations) is applied to help eliminate unrealistic negative peak pressures near leading edges. The method requires an iterative scheme and yields attractive results. There are discrepancies however in the solution method especially using panel or surface singularity distributions which are a function of β ($1/\beta$ to be more exact). First, when determining the effects of other panels on a particular panel (control point), the local β for that particular control point is used, making each panel solution at best a local solution. Putting these solutions together globally is questionable and has not been rationally justified by the author. Second, as the Mach number approaches one (which must occur somewhere on the surface for supersonic flows), $1/\beta$ approaches infinity. To avoid the obvious difficulties this would cause, the author

introduces a correlated local Mach or β (based on calculations for 2-D ramps and cones) for these calculations. Thus while the method yields improved results, it does not rest on the sound theoretical or rational foundation desired before general application.

Objective and Approach

The characteristic feature of all the aforementioned methods is that two distinctly different flow regions in the flowfield about a slender body are clearly evident. One is a region where the perturbations from the free stream conditions are small as assumed in classic thin airfoil or slender body theory. The other region is the stagnation region where these small perturbation assumptions are invalid and produce erroneous results there. The objective of this effort is to develop a method for obtaining uniformly solutions, applicable to arbitrary configurations with round edges in subsonic compressible flow. This of course means that the solution must combine the correct behavior in the stagnation region with that for the remainder of the body while preserving the distinctive nature of each.

Chapter II presents the theoretical development of this new method. The approach is guided by singular perturbation theory in defining these two regions and identifying the appropriate governing equations for each. First and second order problems are formulated including appropriate boundary conditions. The formation of a uniformly valid composite solution synergistically combining the effects of each region

is then proposed based on hypotheses developed in that chapter. Being essentially a perturbation procedure, the resulting method is an approximate method which relies on physical reasoning for understanding many of the steps taken in the development. This is necessarily a consequence of the problem at hand as the exact potential equation is highly nonlinear and adopting some sort of perturbation procedure appears to be the most attractive approach to obtaining reasonable results. This is not to say mathematical rigor is unnecessary, for it will be provided where possible in this development, however: "...the proper questions to ask and approximations to make often come from physical arguments.", (Ref 15).

The application of the method is to elliptic cylinders (2-D) of varying thicknesses in subsonic compressible flow. The ellipse was chosen to test the approach with analytic as opposed to numerical solutions. Chapter III presents the first order analytic solution (Appendix A), application and results. The first order analytic results are compared with the results from thin airfoil theory (Appendix B) and a numerical solution to the exact full potential equation obtained using a Jameson code (Ref 16,17). The first order analytic solution (the first such solution with the stated boundary conditions) is essentially the solution to the Prandtl-Glauert equation with the mass flux surface boundary condition (Ref 18). (A discussion of the mass flux surface boundary condition and its necessity is presented in both Chapters II and

111.) The first order results are shown to compare very favorably with the exact numerical results for thin bodies in subsonic compressible flow.

In Chapter IV the first order method is developed and applied numerically using a current paneling program as developed by Woodward (Ref 2), USSAERO, version B. The purpose of this application is to show that the method can be used with any numerical technique that essentially solves the Prandtl-Glauert equation with the mass flux surface boundary condition, and is not restricted to a specific program. The first application is to a NACA 0012 airfoil (2-D) and the results are compared to the standard paneling results, thin airfoil theory (Appendix C), Jameson results, and experimental data. The second application is to a 3-D glide bomb configuration with the results being compared to the standard paneling results. Calculated inviscid drag is consistently lower than that calculated by standard methods. The new results are thus in better agreement with the theoretically exact value of zero to be expected in subsonic flow. This leads to a higher level of confidence in predicting inviscid drag levels for complex 3-D configurations for later predictions of aerodynamic performance and to the subsequent viscous analysis which is often sensitive to minor changes in pressure gradient. The result is that the proposed method for obtaining uniformly valid solutions about arbitrary configurations, taking into account the effects of the stagnation regions, may be a useful and powerful tool in the aero-

dynamic design of all flight vehicles.

A discussion of the second order problem is presented in Appendix D. A necessary and sufficient condition is presented for the existance of solutions and these solutions are shown to be unique to within an unknown constant. The first order method however remains preferable to a second or higher order effort given the demonstrated accuracy of the first order method and ease of application.

Finally, in Appendix E interesting comparisons of the term $\beta^2\varphi_{xx}+\varphi_{zz}$ as obtained for the 2-D ellipse by various approximations and the exact numerical solution are shown. These comparisons further demonstrate the validity of the first order method in obtaining uniformly valid composite solutions for compressible flow about bodies with round leading or trailing edges.

II Theory

The purpose of this chapter is to provide the theoretical background necessary before general application of the proposed method. The exact problem will be stated for arbitrary configurations in potential flow with a discussion of the surface boundary condition. For motivation of successive steps, a brief order of magnitude analysis will be made for the exact problem. An outer expansion will then be assumed, identified with the region of small disturbances from the free stream conditions for the flow about a slender body. The resulting first and second order approximations to the exact potential equation will then be stated. Next, an inner expansion will be assumed and the resulting first and second order approximations for a stagnation region will be identified. Once general solutions to the inner and outer problems have been obtained, one would classically attempt to match these solutions, ultimately forming a uniformly valid composite solution. This process cannot be accomplished without analytic solutions. Such solutions are non-existent for the general problem (arbitrary configuration) leaving as one alternative, the prospect of numerically patching the outer and inner solutions together. To avoid this prospect the theory developed at this point is reexamined leading to the concept of an intermediate expansion. This expansion is then discussed and the resulting first and second order approximations are identified. With the intermediate expansion the nature of a uniformly valid composite solution is

hypothesized and then formulated. The result is a method that can be applied to any arbitrary configuration with round leading/trailing edges in subsonic potential flow. The first order method as developed can be directly applied using any numerical technique solving the Prandtl-Glauert equation. This versatility leads to a powerful tool for the design process, especially for estimates of that all important performance parameter, drag.

Statement of Exact Problem

The steady inviscid irrotational (potential) flow past an arbitrary configuration (Fig 1) is formulated in terms of the velocity potential $\bar{\Phi}$, where the velocity $\vec{V}=\nabla\bar{\Phi}$, as follows:

$$\nabla^2\bar{\Phi} = \frac{1}{a^2}\left[\vec{V}\cdot\nabla\left(V^2/2\right)\right] \qquad \text{(II-1)}$$

$$\rho\vec{V}\cdot\hat{n} = 0 \quad \text{on surface } F(x,y,z)=0 \qquad \text{(II-2)}$$

$$\nabla\bar{\Phi} \to U_\infty\hat{i} \text{ at infinity} \qquad \text{(II-3)}$$

$$a^2 = a_\infty^2 - \frac{(\gamma-1)}{2}\left(V^2 - U_\infty^2\right) \qquad \text{(II-4)}$$

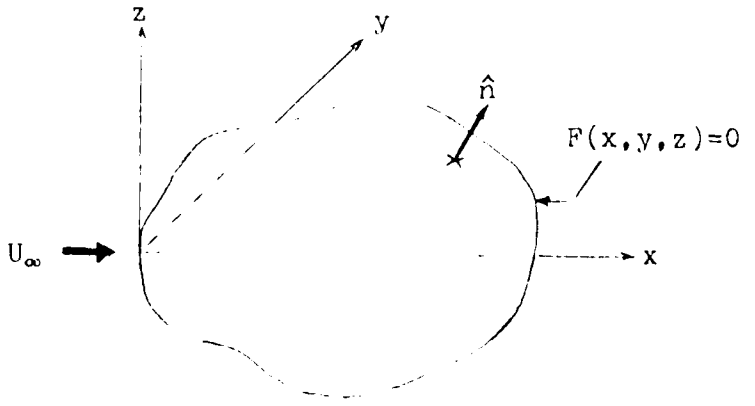

Figure 1. Axis System Notation

As presented here the surface boundary condition differs form the standard velocity boundary condition, $\vec{V}\cdot\hat{n}=0$, by the inclusion of the local density, ρ. It is reasonable to assume that if Eq (II-1) could be solved exactly at every point in the flowfield, then since the density is not zero anywhere, it would suffice to enforce the standard velocity boundary condition at the surface. Equation (II-1) cannot be solved for arbitrary configurations thus one must resort to an approximate method. One approach is to attempt using numerical methods, such as finite difference techniques, to solve Eq (II-1) with the appropriate boundary conditions for a given configuration. For this case it suffices to use the standard velocity boundary condition at the surface as done by Jameson (Ref 16,17). Another approach is to attempt to solve an equation which approximates Eq (II-1). The perturbation technique employed in this report is an example of this latter approach. Equation (II-1) is a mathematical statement that guarantees conservation of mass (continuity equation). An approximation to this equation, such as the Prandtl-Glauert equation, does not assure mass conservation. It has been claimed by Chin (Ref 18) that to obtain analytic solutions to the Prandtl-Glauert equation it is necessary to reinforce this lost continuity condition by imposing the zero mass flux condition at the surface. In fact, it appears impossible to transform the Prandtl-Glauert equation to Laplace's equation and simultaneously maintain a zero net flux condition through the closed-body streamline (Ref 18) when trying to

obtain analytic solutions, unless one uses a consistent approximation (to the approximation implied by the Prandtl-Glauert equation) to the mass flux surface boundary condition. (This is demonstrated in Chapter III as applied to the elliptic cylinder.) For this effort then the mass flux surface boundary condition and approximations thereto will be used throughout. Further demonstration of the validity of using the mass flux surface boundary condition will be shown in Chapter V. Finally, Eq (II-3), is the standard infinity boundary condition requiring any disturbances due to the presence of the body to disappear at fluid infinity.

The exact problem can be restated in terms of a perturbation velocity potential, φ, where

$$\Phi = U_\infty x + \varphi \qquad \text{(II-5)}$$

The gradient of the perturbation velocity potential, $\nabla\varphi$, thus represents the perturbation velocity components, u, v, and w, due to the presence of the body. The problem can now be restated in terms of non-dimensional variables as follows:

$$\bar{\Phi} = U_\infty \ell (\bar{x} + \bar{\varphi}) \qquad \text{(II-6)}$$

$$\bar{\varphi} = \varphi / U_\infty \ell \qquad \text{(II-7)}$$

$$\bar{x} = x/\ell \; ; \; \bar{y} = y/\ell \; ; \; \bar{z} = z/\ell \qquad \text{(II-8)}$$

where ℓ represents some characteristic body length

Replacing the local speed of sound in Eq (II-1) with Eq (II-4) and rewriting Eqs (II-1) through (II-3) in terms of the non-dimensional variables results in the following restatement of the exact problem (dropping the bar notation for non-dimensional quantities):

$$(1-M_\infty^2)\varphi_{xx}+\varphi_{yy}+\varphi_{zz}=M_\infty^2\left[(\gamma+1)\varphi_x+\left(\frac{\gamma+1}{2}\right)\varphi_x^2+\left(\frac{\gamma-1}{2}\right)(\varphi_y^2+\varphi_z^2)\right]\varphi_{xx}+$$
$$M_\infty^2\left[(\gamma-1)\varphi_x+\left(\frac{\gamma-1}{2}\right)\varphi_x^2+\left(\frac{\gamma+1}{2}\right)(\varphi_y^2+\varphi_z^2)\right]\varphi_{yy}+$$
$$M_\infty^2\left[(\gamma-1)\varphi_x+\left(\frac{\gamma-1}{2}\right)\varphi_x^2+\left(\frac{\gamma+1}{2}\right)(\varphi_y^2+\varphi_z^2)\right]\varphi_{zz}+$$
$$2M_\infty^2\left[(\varphi_y+\varphi_x\varphi_y)\varphi_{xy}+(\varphi_z+\varphi_x\varphi_z)\varphi_{xz}+\varphi_y\varphi_z\varphi_{yz}\right] \quad \text{(II-9)}$$

$$(\rho/\rho_\infty)(\vec{V}_{body}\cdot\hat{n})=0 \quad \text{on } F(x,y,z)=0 \quad \text{(II-10)}$$

$$|\nabla\varphi|\to 0 \quad \text{at infinity} \quad \text{(II-11)}$$

Equation (II-9) dramatically shows the highly nonlinear nature of this problem. Analytic solutions for arbitraty configurations cannot be obtained and one is forced to seek numerical or approximate solutions.

Order of Magnitude Observations

Before attempting to develop an approximate solution to Eqs (II-9) through (II-11), some interesting observations can be made by a rudimentary order of magnitude analysis of these exact equations (Ref 7). The classic Prandtl-Glauert equation, which approximates Eq (II-9), results to first order when one assumes that the perturbations due to the body are small:

$$(1-M_\infty^2)\varphi_{xx}+\varphi_{yy}+\varphi_{zz}=0 \quad \text{(II-12)}$$

Equation (II-12) forms the basis for thin airfoil and slender body theories, and for predictive inviscid aerodynamics today. It is valid for slender bodies in subsonic or supersonic potential flows, but as discussed previously yields incorrect results in stagnation regions. If one examines Eq (II-1) or (II-9) for the stagnation region, where $\vec{V}=0$ and $\varphi_x=-U_\infty$ (or -1), to first order Laplace's equation results:

$$\nabla^2\varphi=0 \quad \text{(II-13)}$$

Equation (II-13) describes incompressible potential flow.

This result corresponds with physical intuition as the stagnation region, however small, represents a region where the total velocity and Mach number are approaching zero, thus approaching incompressible (M=0) flow in this region for all free stream Mach numbers. Equation (II-13) while yielding the correct behavior in a stagnation region, is clearly in error when compressibility effects are present for flow over the remainder of the body. Equations (II-12) and (II-13) identify the distinctive nature of the flow about a body by establishing two different regions governed by two different approximations to Eq (II-9) and provide the motivation for further development.

The approach taken will be guided by singular perturbation theory in identifying the nature of these regions and establishing the appropriate order approximations for each. An outer expansion will be assumed associated with the region of small disturbances and first and second order approximations will be developed. This will be followed by the development of an inner expansion associated with the stagnation region. The analysis will be restricted to round edges in subsonic flow as it is felt that no correction is necessary for sharp edges (Ref 11,19). The restriction to subsonic flows is of course a realistic restriction for aerodynamic shapes with round leading edges. The method as developed could also be applied to subsonic round leading edges in supersonic flow.

Outer Expansion

The outer expansion is associated with the region of flow about a body where the assumption of small perturbations from free stream conditions is valid. This is of course, the basic premise of slender body and thin airfoil theory. An outer expansion of the perturbation velocity potential φ, is assumed in terms of a small parameter, ϵ, as follows:

$$\varphi^o = \epsilon \varphi_1^o + \epsilon^2 \varphi_2^o + \cdots \qquad \text{(II-14)}$$

The small parameter, ϵ, can be associated with either the thickness, camber, or angle of attack of the body, whichever is appropriate (Ref 20). (For later applications in Chapters III through V, ϵ will be associated with thickness cases only.) Although it is implied by the form of Eq (II-14) that this series continues indefinitely in powers of ϵ, this has been shown to be not necessarily true (Ref 19). For a round nosed profile (2-D) in subsonic flow, logarithms of ϵ beginning with $\epsilon^4 \ln \epsilon$ appear. This is of no concern for the present development however, as terms beyond the second order will not be used. The assumed expansion for φ^o (Eq II-14) incorporates the correct behavior to be expected when there is no disturbance, or as $\epsilon \to 0$. Substituting Eq (II-14) into Eq (II-9) and gathering like order terms with respect to the parameter ϵ results in the following first and second order approximations to Eq (II-9) for the outer expansion:

$$\epsilon: \quad (1 - M_\infty^2)\varphi_{1_{xx}}^o + \varphi_{1_{yy}}^o + \varphi_{1_{zz}}^o = 0 \qquad \text{(II-15)}$$

$$\epsilon^2: \quad (1 - M_\infty^2)\varphi_{2_{xx}}^o + \varphi_{2_{yy}}^o + \varphi_{2_{zz}}^o = M_\infty^2 \left[(\gamma+1)\varphi_{1_x}^o + (\gamma-1)(\varphi_{1_y}^o + \varphi_{1_z}^o) \right] \varphi_{1_{xx}}^o + 2M_\infty^2 \left[\varphi_{1_y}^o \varphi_{1_{xy}}^o + \varphi_{1_z}^o \varphi_{1_{xz}}^o \right] \qquad \text{(II-16)}$$

Equation (II-15) is the familar Prandtl-Glauert equation as expected, valid for subsonic and supersonic flows.

A surface boundary condition is certainly appropriate for this expansion. Assuming the isentropic expression for ρ/ρ_∞ and small perturbations the mass flux vector can be approximated as follows (Ref 18,21):

$$\frac{\rho}{\rho_\infty}\frac{\vec{V}}{U_\infty} \cong \left(1+\beta^2\frac{u}{U_\infty}, \frac{v}{U_\infty}, \frac{w}{U_\infty}\right)$$

The surface boundary condition, Eq (II-10), then becomes (in terms of φ^0):

$$(1+\beta^2\varphi_x^0)n_x + \varphi_y^0 n_y + \varphi_z^0 n_z = 0 \quad \text{on } F(x,y,z)=0$$

Substituting Eq (II-14) into the preceding equation and gathering like order terms of the parameter ϵ results in the following approximations:

$$\epsilon^0: \; n_x = 0$$

$$\epsilon^1: \; \beta^2\varphi_x^0 n_x + \varphi_y^0 n_y + \varphi_z^0 n_z = 0$$

$$\epsilon^2: \; \beta^2\varphi_x^1 n_x + \varphi_y^1 n_y + \varphi_z^1 n_z = 0$$

The zeroeth order approximation (ϵ^0) represents a flat plate at zero angle of attack, or no disturbances ($\epsilon=0$), as expected. Now, if the surface is described by

$$F(x,y,z) = \epsilon f(x) + g(y,z) = 0$$

where

$$n_x = \epsilon\frac{\partial f}{\partial x}/|\nabla F|, \quad n_y = \frac{\partial g}{\partial y}/|\nabla F|, \quad n_z = \frac{\partial g}{\partial z}/|\nabla F|$$

we have the description of a slender body at zero angle of attack with ϵ representing the maximum thickness. The surface boundary condition now becomes:

$$\epsilon^1: \; \varphi_x^0\frac{\partial f}{\partial x} + \varphi_y^0\frac{\partial g}{\partial y} + \varphi_z^0\frac{\partial g}{\partial z} = 0$$

$$\epsilon^2: \; \beta^2\varphi_x^1\frac{\partial f}{\partial x} + \varphi_{2y}^0\frac{\partial g}{\partial y} + \varphi_{2z}^0\frac{\partial g}{\partial z} = 0$$

For 2-D flows the first order approximation yields

$$\varphi_z^1 = -\frac{\partial f}{\partial x}\Big/\frac{\partial g}{\partial z} \quad \text{on } F(x,z)=0$$

For configurations with round leading edges, $\frac{\partial F}{\partial x} = \pm\infty$ at the stagnation point and thus q_1^0 would be undefined in this region for this approximation. It is proposed then that the zeroeth and first order equations of the original approximation be combined as follows:

$$(1+\epsilon\beta^2 q_1^0)n_x + \epsilon q_2^0 n_y + \epsilon q_3^0 n_z = 0 \quad \text{on } F(x,y,z)=0 \qquad \text{(II-17)}$$

This then forms the first order surface boundary condition and is similar to that developed by Chin (Ref 18). The second order surface boundary condition approximation is then given by:

$$\beta^2 q_1^0 n_x + q_2^0 n_y + q_3^0 n_z = 0 \quad \text{on } F(x,y,z)=0 \qquad \text{(II-18)}$$

Note that from the form of the first order equation, Eq (II-17), one can infer immediately that the stagnation point velocity will not be zero for a non-lifting body in other than incompressible flow ($M_\infty=0$ or $\beta=1$). This again confirms previous statements that the outer solution is in error in this region.

The infinity boundary condition is also appropriate for this expansion and is that the disturbances due to the presence of the body disappear to first and second order at fluid infinity:

$$|\vec{q}_1^0| \to 0 \quad \text{at infinity} \qquad \text{(II-19)}$$

$$|\vec{q}_2^0| \to 0 \quad \text{at infinity} \qquad \text{(II-20)}$$

Inner Expansion

Before assuming an inner expansion associated with the stagnation region, the dependent and independent variables previously defined are strained (Ref 10,19) to magnify this

region where the outer expansion is invalid. Research has shown that no correction is necessary for sharp edges, corrections will be made only for round edges where the associated radius is proportional to ϵ^2 (Ref 19). Let $\delta = \epsilon^2$ be the parameter used to strain the dependent and independent variables as follows:

$$\bar{\varphi} = \varphi/\delta \; ; \; \bar{x} = x/\delta \; ; \; \bar{y} = y/\delta \; ; \; \bar{z} = z/\delta \qquad \text{(II-21)}$$

Equation (II-9) remains unchanged in terms of the new variables. An inner expansion, $\bar{\varphi}'(\bar{x},\bar{y},\bar{z})$, is then assumed in powers of δ where,

$$\bar{\varphi}' = -\bar{x} + \delta\bar{\varphi}_1' + \delta^2\bar{\varphi}_2' + \cdots \qquad \text{(II-22)}$$

The reason for this choice becomes clear as one sees that as the disturbance parameter, δ, approaches zero (flat plate at zero angle of attack), the total velocity approaches zero or stagnation point conditions as desired. Substituting Eq (II-22) into Eq (II-9) in terms of the new variables results in the following first and second order approximations:

$$\delta^1: \nabla^2\bar{\varphi}_1' = 0 \qquad \text{(II-23)}$$

$$\delta^2: \nabla^2\bar{\varphi}_2' = 0 \qquad \text{(II-24)}$$

(The Laplacian operator denoting operations with respect to $\bar{x}$, $\bar{y}$, and $\bar{z}$.) Rewriting Eqs (II-23) and (II-24) in terms of the original variables results in the following:

$$\delta^1: \nabla^2\varphi_1' = 0 \qquad \text{(II-25)}$$

$$\delta^2: \nabla^2\varphi_2' = 0 \qquad \text{(II-26)}$$

(The Laplacian operator now denoting operations with respect to x, y, and z.) Equations (II-25) and (II-26) again confirm physical intuition and the order of magnitude analysis

presented earlier that the flow in the stagnation region can be approximated as being incompressible, even to second order (this is not true for higher order approximations). This implies that a solution can be obtained independent of free stream conditions once the shape is specified, for subsonic through supersonic flows (assuming the appropriate boundary conditions have been specified).

A surface boundary condition is also appropriate for this region. To second order, an expansion of ρ/ρ_∞ from stagnation conditions is a constant as expected. Since the flow in this region is being approximated by incompressible flow (M=0), the surface boundary condition is identical to the velocity boundary condition at the surface (written in outer variables):

$$(1+\varepsilon\phi_{x_1})\phi_{x_1} + \varepsilon\phi_{y_1}\phi_{x_1} + \varepsilon\phi_{z_1}\phi_{x_1} = 0 \qquad \text{on } F(x,y,z)=0$$

Substituting Eq (II-22) into the preceding equation in terms of inner variables and gathering like order terms of the parameter δ results in the following first and second order surface boundary condition approximations (written in outer variables):

$$\nabla\phi_1 \cdot \hat{n} = 0 \qquad \text{on } F(x,y,z)=0 \qquad \text{(II-27)}$$

$$\nabla\phi_2 \cdot \hat{n} = 0 \qquad \text{on } F(x,y,z)=0 \qquad \text{(II-28)}$$

Summary

As noted earlier the outer solution, once obtained, is valid everywhere about a slender body or thin airfoil except in the stagnation region. An inner solution would of course be valid only in the stagnation region. It appears attractive

and desirable to combine these two solutions, retaining the essential features of each, forming a uniformly valid composite solution. Classically this would be done (to first order for example) by first solving the outer problem given by Eq (II-15) with boundary conditions given by Eqs (II-17) and (II-19); and, the inner problem given by Eq (II-25) with the boundary condition given by Eq (II-27) to within an unknown function. Next, the solutions would be matched (Ref 19) to determine the remaining boundary condition and form a uniformly valid composite solution. This composite solution is obtained by summing the outer and inner problems or solutions to appropriate order and subtracting their common limit. This process requires analytic solutions and as mentioned previously, such solutions are nonexistent for applications to arbitrary configurations. The remaing alternative is to numerically patch the two solutions together. As the first approach is not plausible, this approach is not desirable. The problem remains: how to form a uniformly valid solution in a reasonable manner. Before accomplishing this however, the ability to match outer and inner solutions assumes that their respective domains of validity overlap. There is no reason a priori to assume that this is true and in fact for some applications they may not overlap (Ref 19).

Intermediate Expansion

To bridge the gap that may exist between outer and inner domains of validity it is necessary to consider an intermediate expansion, a concept developed mainly by Kaplun (Ref

19,22). It was introduced in part to try and formally explain why the classical method of matching solutions worked in cases where it should not, and did not work in cases where it should. Kaplun's Extension Theorem (Ref 19,22) attempts to formally define the matching process through defining and extending, if necessary, regions or domains of validity by using the intermediate expansion. This attempt is viewed as heuristic by some (Ref 19). To begin, the dependent and independent variables are again strained as follows:

$$\tilde{\varphi} = \varphi/\epsilon^{A} \; ; \; \tilde{x} = x/\epsilon^{A} \; ; \; \tilde{y} = y/\epsilon^{A} \; ; \; \tilde{z} = z/\epsilon^{A} \qquad \text{(II-29)}$$

Equation (II-9) remains unchanged in terms of the new variables. Letting $\tau = \epsilon\epsilon^{1/2}$ an intermediate expansion, $\tilde{\varphi}^{I}(\tilde{x},\tilde{y},\tilde{z})$, is assumed as follows:

$$\tilde{\varphi}^{I} = -\frac{A}{2}\tilde{x} + \tau\tilde{\varphi}_{1}^{I} + \tau^{2}\tilde{\varphi}_{2}^{I} + \cdots \qquad \text{(II-30)}$$

The reason for this choice can be clearly seen since for A=0 the outer variables result, while for A=2 the inner variables and expansion result. Thus A is assumed to be some undetermined constant between zero and two, i.e.,

$$0 < A < 2 \qquad \text{(II-31)}$$

This expansion can be physically interpretted as an expansion from $[(2-A)U_{\infty}]/2$ while the outer expansion is from U_{∞}, and the inner expansion is from a zero stagnation point velocity. Substituting Eq (II-30) into Eq (II-9) in terms of the new variables results in the following first and second order approximations (rewritten in the original variables):

$$\tau: \Delta\varphi_{xx}^{I} + \varphi_{yy}^{I} + \varphi_{zz}^{I} = 0 \qquad \text{(II-32)}$$

$$\Delta = \left\{(1-M_{\infty}^{2}) + \tfrac{1}{2}A(\gamma+1)M_{\infty}^{2}\left(1-\tfrac{A}{4}\right)\right\} \Big/ \left\{1 + \tfrac{1}{2}A(\gamma-1)M_{\infty}^{2}\left(1-\tfrac{A}{4}\right)\right\}$$

$$\tau^2: \Delta\varphi^I_{xx} + \varphi^I_{yy} + \varphi^I_{zz} = A_1[(\gamma+1)\varphi^I_x\varphi^I_{xx} + (\gamma-1)(\varphi^I_y\varphi^I_{yy} + \varphi^I_z\varphi^I_{zz})] +$$
$$2A_1^2[\varphi^I_x\varphi^I_{xy} + \varphi^I_y\varphi^I_{yz} + \varphi^I_z\varphi^I_{xz}] \qquad (II-33)$$
$$A_1 = M_\infty^2(1-A)/[1+\tfrac{1}{2}A(\gamma-1)M_\infty^2(1-A)]$$

Again note that for A=0 the outer equations result while for A=2 the inner equations result.

A surface boundary condition also seems appropriate for this region. Physically, the first order intermediate approximation, Eq (II-32), appears to be flow at a Mach number defined by $M_I=\sqrt{1-\Delta}$, since Δ appears in the same position as β^2 in Eq (II-15) for the outer approximation ($\Delta=\beta^2$ for A=0). Based on this analogy the surface boundary condition for the intermediate approximation is assumed to be:

$$(1+\lambda\varphi^I_x)n_x + \varphi^I_y n_y + \varphi^I_z n_z = 0 \qquad \text{on } F(x,y,z)=0$$

In terms of the outer variables the first and second order boundary condition approximations then are:

$$[(1-\tfrac{A}{2}\Delta)+2\lambda\varphi^I_x]n_x + 2\varphi^I_y n_y + 2\varphi^I_z n_z = 0 \qquad \text{on } F(x,y,z)=0 \qquad (II-34)$$

$$\Delta\varphi^I_x n_x + \varphi^I_y n_y + \varphi^I_z n_z = 0 \qquad \text{on } F(x,y,z)=0 \qquad (II-35)$$

Note, as before, that for A=0 the outer equations result while for A=2 the inner equations result. Now by using the intermediate expansion and applying Kaplun's Extension Theorem (Ref 22), the inner and outer solutions may be formally matched. This is accomplished essentially by extending the domains of validity of each (if necessary) and choosing A such that these domains overlap. As before, however, this is a process which appears to require analytic solutions.

Hypotheses

The problem remains as to how to form a uniformly valid

composite solution. To avoid numerical patching it is necessary to somehow determine the common limit required to form this composite solution. Consider the following quotes with respect to the composite solution and intermediate expansion:

> "Composite solution...the sum of the inner and outer expansions is corrected by the part they have in common (Ref 19:94)."
>
> "Intermediate expansion...in some overlap domain the intermediate expansion of the difference between the outer (or inner) expansion must vanish to appropriate order (Ref 19:92)."

In light of the essence of these statements and the inherent nature of the intermediate expansion with respect to the outer or inner expansions, the following hypothesis is proposed:

i. The solution to the intermediate expansion is, to sufficient order, the common limit necessary for matching.

With this hypothesis, a composite solution can now be formed. However, the inner and intermediate problems cannot as yet be fully solved as they lack a necessary boundary condition. Furthermore, for application to current numerical methods, it would be desirable to have each problem (outer, inner, and intermediate) be independent, well posed and unique to a given configuration. Each solution contributing to the formation of a uniformly valid composite solution as to be demonstrated. Since the nature of this problem is a uniform stream perturbed by a body whose disturbances must disappear at infinity, a final hypothesis is proposed:

ii. The remaining boundary condition for the inner and intermediate problems is that disturbances due to the body disappear at fluid infinity.

With hypotheses (i) and (ii) three well posed problems are defined, each of which can be solved independently for the same configuration, such that each solution contributes to a uniformly valid composite solution.

Composite Solution

As previously stated, the composite solution is the sum of the outer and inner solutions minus the part they have in common. As hypothesized, this common limit is the intermediate solution for a given value of A. The resultant velocities for each solution, being directly a function of the individual perturbation potential functions, will then be calculated and used to form the composite solution (Ref 19). The use of the respective velocities to form the composite solution is a matter of choice as a composite could just as easily be formed in terms of the perturbation potential φ. The individual velocities however, are more definitive in terms of physical significance as well as being direct inputs to any aerodynamic calculations. The velocities for each region in terms of the perturbation potentials for the respective expansions are given by the following:

$$\frac{\vec{V}^o}{U_\infty} = (1 + q_x^o, q_y^o, q_z^o)$$

$$\cong (1 + \varepsilon q_x^o + \varepsilon^2 q_x^o, \varepsilon q_y^o + \varepsilon^2 q_y^o, \varepsilon q_z^o + \varepsilon^2 q_z^o) \qquad \text{(II-36)}$$

$$\frac{\vec{V}^i}{U_\infty} = (1 + q_x^i, q_y^i, q_z^i)$$

$$\cong (1 + \delta' q_x^i + \delta'^2 q_x^i, \delta' q_y^i + \delta'^2 q_y^i, \delta' q_z^i + \delta'^2 q_z^i) \qquad \text{(II-37)}$$

$$\frac{\vec{V}^I}{U_\infty} = (1 + q_x^I, q_y^I, q_z^I)$$

$$\cong (1 - \frac{A}{2} + \varepsilon q_x^I + \varepsilon^2 q_x^I, \varepsilon q_y^I + \varepsilon^2 q_y^I, \varepsilon q_z^I + \varepsilon^2 q_z^I) \qquad \text{(II-38)}$$

The composite solution may be formed by either of two combi-

nations (Ref 19) of the resultant velocities from each region as follows (note that for incompressible flow, $M_\infty=0$, both rules yield the same result as desired):

(additive) $$\left.\frac{V}{u_\infty}\right|_c = \left.\frac{V}{u_\infty}\right|_o + \left.\frac{V}{u_\infty}\right|_i - \left.\frac{V}{u_\infty}\right|_t \qquad \text{(II-39)}$$

(multiplicative) $$\left.\frac{V}{u_\infty}\right|_c = \left\{\left(\left.\frac{V}{u_\infty}\right|_o\right)\left(\left.\frac{V}{u_\infty}\right|_i\right)\right\} \Big/ \left(\left.\frac{V}{u_\infty}\right|_t\right) \qquad \text{(II-40)}$$

In terms of the surface velocity, the multiplicative composite solution is preferred, as it has been shown (Ref 19,23) to give better results in the stagnation region (this is easily seen by the fact that the multiplicative composition results in a zero velocity at the stagnation point for all free stream Mach numbers). Note however, that in using the multiplicative composition, the possibility exists for the intermediate solution to equal zero, thus resulting in a singular point. This has been shown (ref 23) to occur in the flowfield and not on the surface, and will be verified later analytically.

Summary

The following is a summary of the first and second order approximations for each expansion as developed in this chapter.

i. Outer Expansion:

$$\beta^2 \phi^o_{xx} + \phi^o_{yy} + \phi^o_{zz} = 0 \qquad \text{(II-41)}$$

$$(1 + (\gamma-1)\phi^o_x)n_x + \phi^o_y n_y + \phi^o_z n_z = 0 \quad \text{on } F(x,y,z)=0 \qquad \text{(II-42)}$$

$$|\nabla \phi^o| \to 0 \quad \text{at infinity} \qquad \text{(II-43)}$$

$$\beta^2 \phi^i_{xx} + \phi^i_{yy} + \phi^i_{zz} = M_\infty^2\{(\gamma+1)\phi^o_x\phi^o_{xx} + (\gamma-1)(\phi^o_y\phi^o_{yy} + \phi^o_z\phi^o_{zz})\}\phi^o_x + 2M_\infty^2\{\phi^o_y\phi^o_{xy} + \phi^o_z\phi^o_{xz}\} \qquad \text{(II-44)}$$

$$\beta^2 \phi^t_x n_x + \phi^t_y n_y + \phi^t_z n_z = 0 \quad \text{on } F(x,y,z)=0 \qquad \text{(II-45)}$$

$$|\nabla \phi^t| \to 0 \quad \text{at infinity} \qquad \text{(II-46)}$$

ii. Inner Expansion:

$$\nabla^2 \phi_1^I = 0 \tag{II-47}$$

$$\nabla \phi_1^I \cdot \hat{n} = 0 \quad \text{on } F(x,y,z)=0 \tag{II-48}$$

$$\phi_1^I \to A_{11}, (\phi_{1y}^I, \phi_{1z}^I) \to 0 \quad \text{at infinity} \tag{II-49}$$

$$\nabla^2 \phi_2^I = 0 \tag{II-50}$$

$$\nabla \phi_2^I \cdot \hat{n} = 0 \quad \text{on } F(x,y,z)=0 \tag{II-51}$$

$$|\nabla \phi_2^I| \to 0 \quad \text{at infinity} \tag{II-52}$$

iii. Intermediate Expansion:

$$\beta^2 \phi_{1xx}^I + \phi_{1yy}^I + \phi_{1zz}^I = 0 \tag{II-53}$$

$$\left[(1-\tfrac{A}{2}\lambda) + \lambda_2 \phi_{1x}^I\right] n_x + \phi_{1y}^I n_y + \phi_{1z}^I n_z = 0 \quad \text{on } F(x,y,z)=0 \tag{II-54}$$

$$\phi_{1x}^I \to A_{11}, (\phi_{1y}^I, \phi_{1z}^I) \to 0 \quad \text{at infinity} \tag{II-55}$$

$$\beta^2 \phi_{2xx}^I + \phi_{2yy}^I + \phi_{2zz}^I = \lambda_1 \left\{(\gamma+1)\phi_{1x}^I + (\gamma-1)(\phi_{1y}^I + \phi_{1z}^I)\right\} \phi_{1x}^I + 2\lambda_1 \left\{\phi_{1y}^I \phi_{1xy}^I + \phi_{1z}^I \phi_{1xz}^I\right\} \tag{II-56}$$

$$\beta^2 \phi_{2x}^I n_x + \phi_{2y}^I n_y + \phi_{2z}^I n_z = 0 \quad \text{on } F(x,y,z)=0 \tag{II-57}$$

$$|\nabla \phi_2^I| \to 0 \quad \text{at infinity} \tag{II-58}$$

The composite solution, in terms of resultant velocities, is formed according to Eq (II-39) or (II-40). It is interesting to note that all the first order problems as stated can be solved using current numerical techniques, such as panel methods (Ref 5), which solve the Prandtl-Glauert equation subject to mass flux surface boundary conditions. The outer problem would be solved for the free stream Mach number, the inner problem for a zero Mach number (incompressible), and the intermediate problem for some intermediate Mach number, M_I, as determined by the value of A. The more exact and uniformly valid composite solution would then be formed as specified making the first order method a very powerful yet simple

technique for application to arbitrary configurations in subsonic potential flow.

III First Order Application: Elliptic Cylinder in Subsonic Compressible Flow

The purpose of this chapter is to describe the detailed results obtained by applying the first order approximation, as developed in Chapter II, to a nonlifting elliptic cylinder (2-D ellipse) in subsonic compressible flow. The elliptic cylinder was chosen for application so that analytic rather than numerical results could be used to test the method for a variety of thicknesses and Mach numbers. The problem will be stated with the surface mass flux boundary condition and an analytic solution will be presented. Details of the solution are in Appendix A. This is the first such solution, to this author's knowledge, with the prescribed boundary conditions. The necessity for the mass flux boundary condition will also be demonstrated as promised earlier. Surface velocities will be evaluated for an ellipse with a ten percent maximum thickness to chord ratio at a free stream Mach number of 0.5. This case will be used to depict the various aspects of the proposed method and solutions, and show that the multiplicative composition is preferred to the additive composition for representation of surface velocities. No attempt will be made to optimize the value of A, Eq (II-31), and unless otherwise stated, the value of A will be one for all applications. Finally, the first order multiplicative composite results will be compared to results from thin airfoil theory (Appendix B) and numerical results obtained from a Jameson code (Ref 16,17) which solves the exact poten-

tial equation (Eq (11-9) with the velocity surface boundary condition and the standard infinity boundary condition). Comparisons will be made of total surface velocity and surface velocity perturbation components (u and w) for a variety of thicknesses and Mach numbers. The comparisons will show that the uniformly valid first order solutions compare very favorably with the exact numerical solutions within the limits of validity of the theory, that is, for thin bodies at subsonic Mach numbers. The composite results do not compare favorably at transonic Mach numbers or for thick bodies in subsonic or transonic flow.

Statement of Problem

For application of the first order method, consider a nonlifting elliptic cylinder (Fig 2) in the subsonic compressible isentropic flow (potential flow) of a perfect gas (γ=1.4), whose surface is given by

$$F(x,z) = x^2 + \left(\frac{z}{\epsilon}\right)^2 - 1 = 0 \qquad \text{(III-1)}$$

Here the parameter ϵ is the maximum thickness to chord ratio.

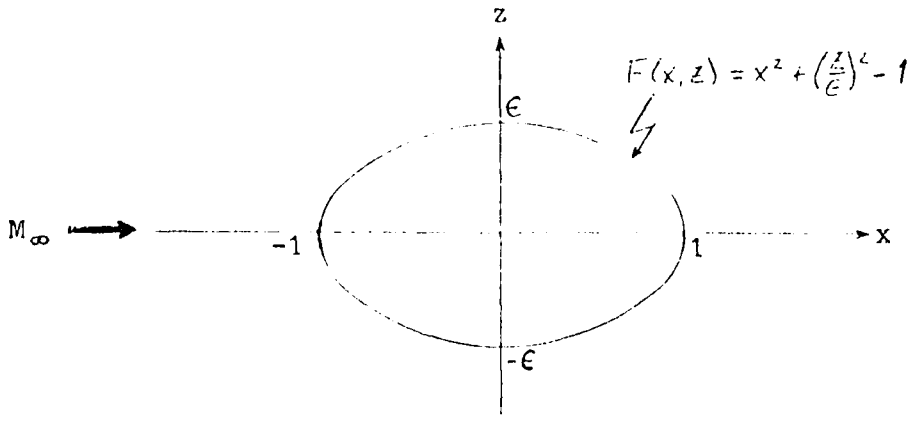

Figure 2. Elliptic Cylinder

The outer, inner, and intermediate first order problems are all of the form

$$B^2\varphi_{xx} + \varphi_{zz} = 0 \qquad \text{(III-2)}$$

$$\left[\left(1-\frac{A}{2}B^2\right)+\varepsilon B^2\varphi_x\right]x + \varepsilon\varphi_z\left(\frac{z}{\varepsilon}\right) = 0 \quad \text{on } F(x,z)=0 \qquad \text{(III-3)}$$

$$\varphi_x \to A/2\,z\,,\ \varphi_z \to 0 \quad \text{at infinity} \qquad \text{(III-4)}$$

where

$$B^2 = \begin{cases} \beta^2, \text{ outer } (A=0),\ z=\epsilon \\ \Delta, \text{ intermediate } (0<A<2),\ z=\epsilon\epsilon^{A/2} \\ 1, \text{ inner } (A=2),\ z=\epsilon^2 \end{cases} \qquad \text{(III-5)}$$

Equation (III-2) with boundary conditions given by Eqs (III-3) and (III-4) states the first order problem for an elliptic cylinder. The specific approximation is determined by the value of A, Eq (III-5).

Method of Solution

The solution method (details in Appendix A) for obtaining analytic results for the first order problem requires transformation of the problem to a known solution, incompressible flow about a circular cylinder. This involves first transforming the problem to incompressible flow about an equivalent elliptic cylinder with the transformations $\bar{x}=x/B$, $\bar{\varphi}=B\varepsilon\varphi$, and $\bar{\bar{\Phi}}=(1-\frac{A}{2}B^2)\bar{x}+\bar{\varphi}$ resulting in:

$$\bar{\bar{\Phi}}_{\bar{x}\bar{x}} + \bar{\bar{\Phi}}_{zz} = 0 \qquad \text{(III-6)}$$

$$\bar{\bar{\Phi}}_{\bar{x}}(B^2\bar{x}) + \bar{\bar{\Phi}}_z\left(\frac{z}{\varepsilon}\right) = 0 \quad \text{on } F(x,z)=0 \qquad \text{(III-7)}$$

$$\bar{\bar{\Phi}}_{\bar{x}} \to 1\,,\ \bar{\bar{\Phi}}_z \to 0 \quad \text{at infinity} \qquad \text{(III-8)}$$

where

$$F(\bar{x},z) = (B\bar{x})^2 + \left(\frac{z}{\varepsilon}\right)^2 - 1 = 0 \qquad \text{(III-9)}$$

Once this is accomplished, the problem is then mapped using elliptic coordinates to the known solution. The mapping

function used is the well known Joukowski transform. The resulting first order analytic solution is then,

$$\phi(x,y) = \frac{kQ}{2B\epsilon}\left\{\theta + \sqrt{\theta^2-1}\right\}\left\{1+\epsilon^2\right\} - \left(1-\frac{A\epsilon^2}{2}\right)\frac{x}{2B} + \text{constant} \qquad \text{(III-10)}$$

where

$$k = \frac{1}{B}\sqrt{1-(B\epsilon)^2} \qquad \text{(III-11)}$$

$$\theta = P + \ell/2k \qquad \text{(III-12)}$$

$$\Omega = P - \ell/2k \qquad \text{(III-13)}$$

$$R = \sqrt{\frac{1+B\epsilon}{1-B\epsilon}}\Big/\left(\theta + \sqrt{\theta^2-1}\right) \qquad \text{(III-14)}$$

$$P = \sqrt{z^2 + (x/B + k)^2} \qquad \text{(III-15)}$$

$$q = \sqrt{z^2 + (x/B - k)^2} \qquad \text{(III-16)}$$

and

$$u/u_\infty = \phi_x \,, \quad w/u_\infty = \phi_z \qquad \text{(III-17)}$$

$$V/u_\infty = \sqrt{(1+u/u_\infty)^2 + (w/u_\infty)^2} \qquad \text{(III-18)}$$

For a given free stream Mach number, M_∞, and maximum thickness to chord ratio, ϵ, the velocities for each solution can be evaluated with A=0 for the outer solution, A=2 for the inner solution, and an assumed value of A (A=1) for the intermediate solution. The velocities for the composite solution are then determined using either Eq (II-39) or (II-40).

Let us now determine what would have happened if the standard velocity surface boundary condition, and not Eq (III-3), had been applied. Consider the following restatement of the problem with the velocity boundary condition, V n=0, being applied at the surface. The infinity boundary condition is not affected.

$$B^2\phi_{xx} + \phi_{zz} = 0$$

$$\left(1 - \frac{A}{2} + 2\phi_x\right)x + 2\phi_z\left(z/B\right) = 0 \qquad \text{(III-19)}$$

(Note that a zero stagnation point velocity is enforced as a consequence of using Eq (III-19) for all free stream Mach numbers for the outer approximation, A=0. We must ask if this is a reasonable result of a method based on small perturbations, outer approximation, for compressible flow.)

The standard Prandtl-Glauert transformation, $x=B\bar{x}$, is applied resulting in,

$$\begin{aligned} &\varphi_{\bar{x}\bar{x}} + \varphi_{zz} = 0 \\ &\left(1 - \frac{A}{2} + \frac{\tau}{B}\varphi_{\bar{x}}\right) B\bar{x} + \tau\varphi_{z}\left(\frac{z}{c}\right) = 0 \end{aligned} \qquad \text{(III-20)}$$

Now let $\varphi = \frac{B}{c}\bar{\varphi}$ and $\bar{\Phi} = \left(1 - \frac{A}{2}\right)\bar{x} + \bar{\varphi}$ resulting in

$$\begin{aligned} &\bar{\Phi}_{\bar{x}\bar{x}} + \bar{\Phi}_{zz} = 0 \\ &\bar{\Phi}_{\bar{x}}(\bar{x}) + \bar{\Phi}_{z}\left(\frac{z}{c}\right) = 0 \end{aligned} \qquad \text{(III-21)}$$

As before, the problem has been successfully transformed to the incompressible flow case, but now the surface boundary condition is being satisfied on

$$\bar{F}(\bar{x}, z) = \bar{x}^2 + (z/c)^2 - 1 = 0 \qquad \text{(III-22)}$$

or

$$\bar{F}(x, z) = (x/B)^2 + (z/c)^2 - 1 = 0 \qquad \text{(III-23)}$$

and not on the specified surface, $F(x,z)=0$, given by Eq (III-1). Thus while one may obtain a solution that appears correct, since both surfaces have the same maximum thickness (only the chord lengths are different) and yield approximately the same maximum velocity, it is clearly for the wrong surface. In fact, this problem cannot be successfully transformed to an equivalent incompressible flow problem for the same or given surface using the velocity boundary condition (Ref 18). Recall that thin airfoil theory neglects the x-

component of perturbation velocity and thus this problem does not arise. This results for any surface and is not peculiar to the ellipse.

Analytic Results

Analytic results of the first order method will now be presented and discussed for the 2-D ellipse. The results are for an ellipse with a ten percent maximum thickness to chord ratio at a free stream Mach number of 0.5. All data is for the nonlifting problem only.

Figure 3 shows the surface velocity comparisons for the outer, inner, and intermediate (A=1) solutions. These three solutions of course contribute to the composite solution. In Fig 3 it is clearly seen that the outer solution is in error at the stagnation point. The inner solution, although correct at the stagnation point, does not include the effects of compressibility as represented by the outer solution for the remainder of the body. The intermediate solution is seen to be in error for both of these regions. None of these individual solutions represents a solution that can be considered uniformly valid for the entire body.

Figure 4 presents the surface velocity comparisons for the outer, inner, and multiplicative composite (A=1) solutions. Here it is seen that the composite solution combines the compressibility of the outer solution with a zero stagnation point velocity representative of the inner solution. The composite solution transitions smoothly from the inner to the outer solution, combining the effects of both. The tran-

sition occurs very close to the stagnation point, confirming the fact that the outer solution, or Prandtl-Glauert solution, is the dominant solution (and as previously discussed, a very good approximation, borne out by its common use, except in the stagnation region). The pertinent result in this figure, however, is that the composite solution represents a uniformly valid solution about a thin body with blunt edges.

Figure 5 shows the effect when using the additive composite solution on the surface velocity due to varying the value of A (A=0.5,1.0,1.5). As A increases more of the effect of the inner solution is being subtracted from the composite solution, and the composite solution moves toward the outer solution as shown. The difference between the solutions for the different values of A is negligible except at and near the stagnation point. The additive composition was used here to illustrate these effects and also to show why the multiplicative composition is preferred since a zero stagnation point velocity results from the multiplicative composition for all values of A. This comparison between the additive and multiplicative compositions is shown in Fig 6 for a value of A=1. As shown in this figure the solutions are identical except at and near the stagnation point. These figures suggest that there may be some optimum or desired value of A for forming the composite solution, however, this requires some other criteria than has been presented (such as experimental data). Without such guidance, it appears

that a value of A=1 should suffice for most applications.

As mentioned earlier, the possibility exists, when using the multiplicative composition, that the intermediate solution may equal zero at some point yielding a singular solution at this point. This does indeed occur, as shown in Fig 7, but always occurs in the flowfield and not on the surface (Ref 23). This demonstrates that although the multiplicative composition is preferred for evaluating surface velocities, care must be taken when using this composition in the flowfield. The additive composition does not have any singular points.

The purpose of the figures presented to this point has been to show that the three first order analytic solutions (outer, inner, intermediate) can be successfully combined into a uniformly valid solution. This composite solution correctly combines compressibility effects (represented by the outer solution) with the correct flow behavior in the stagnation region (represented by the inner solution) for a thin body with blunt edges in subsonic flow. The composite solution is formed by combining these two solutions being sure to subtract their common limit (represented by the intermediate solution for a fixed value of A). The three solutions are essentially solutions to the Prandtl-Glauert equation for $M=M_\infty$ (outer solution), and $M=M_I$ (intermediate solution where $M_\infty < M_I < 0$), and M=0 (inner solution), for the given surface and infinity boundary conditions. In terms of surface velocities the multiplicative composition has been shown

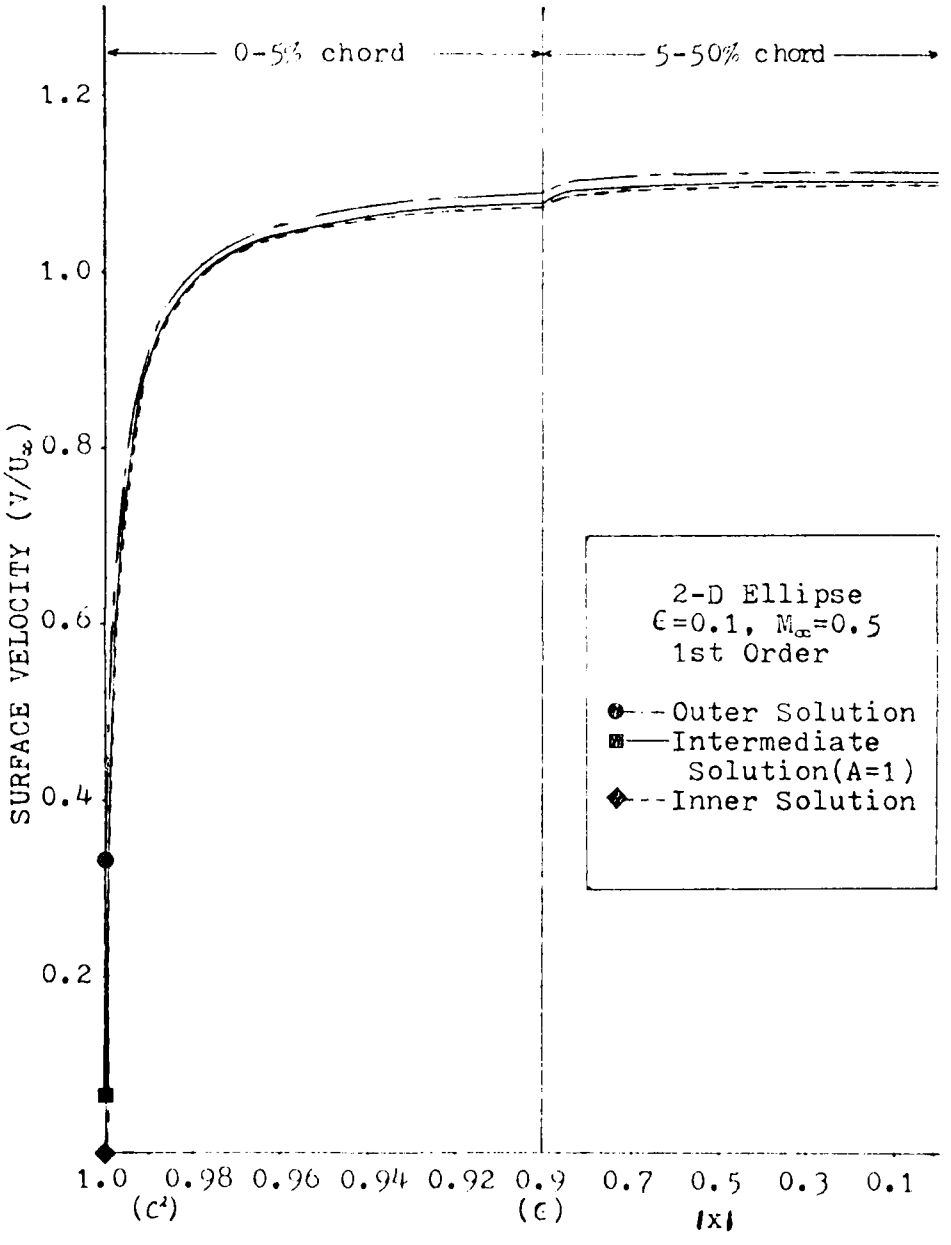

Figure 3. First Order Surface Velocity Comparisons, Outer, Inner, and Intermediate (A=1) Analytic Solutions, 2-D Ellipse, $\epsilon=0.1$, $M_\infty=0.5$, 0-50% Chord

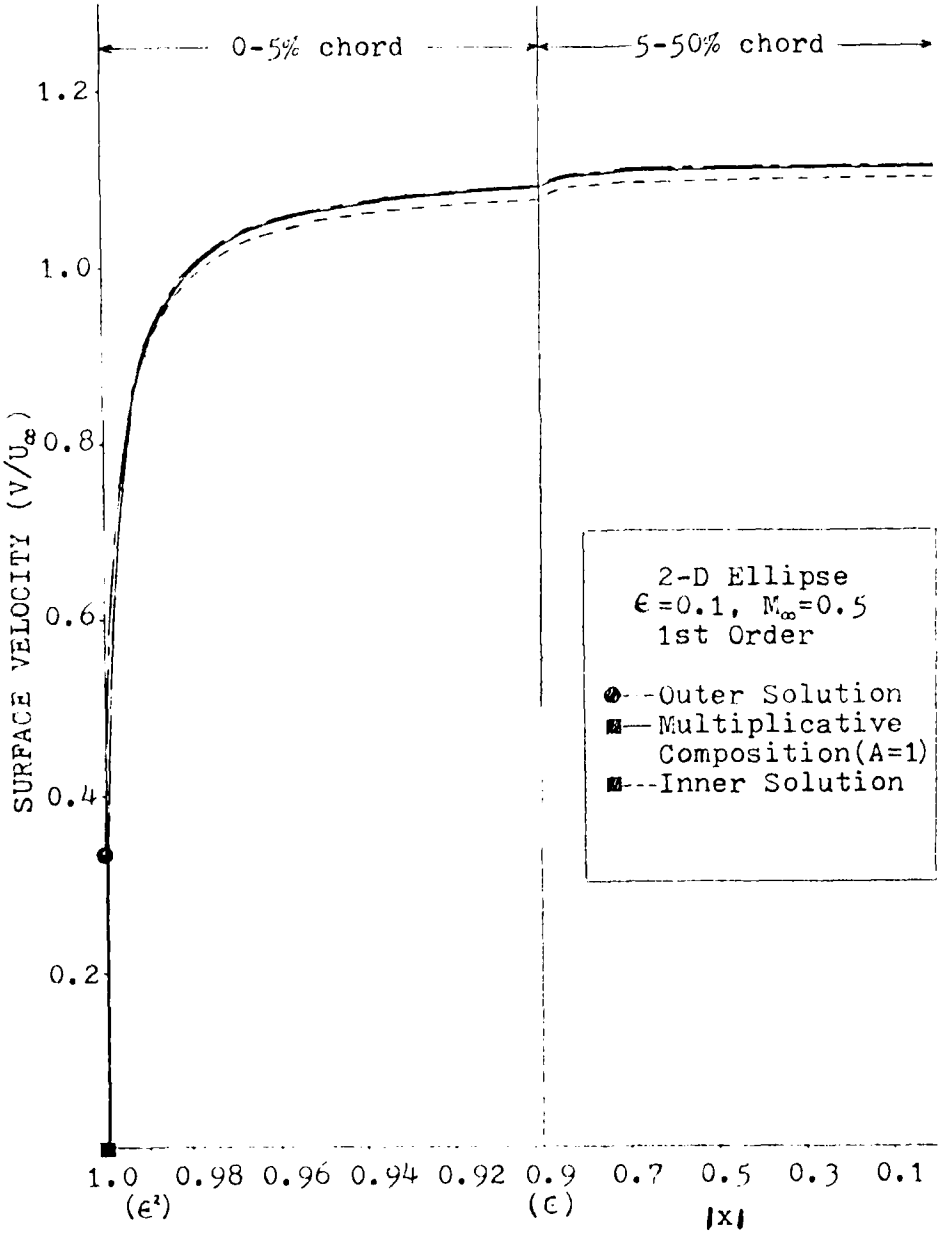

Figure 4. First Order Surface Velocity Comparisons, Outer, Inner, and Multiplicative Composite (A=1) Analytic Solutions, 2-D Ellipse, $\epsilon=0.1$, $M_\infty=0.5$, 0-50% Chord

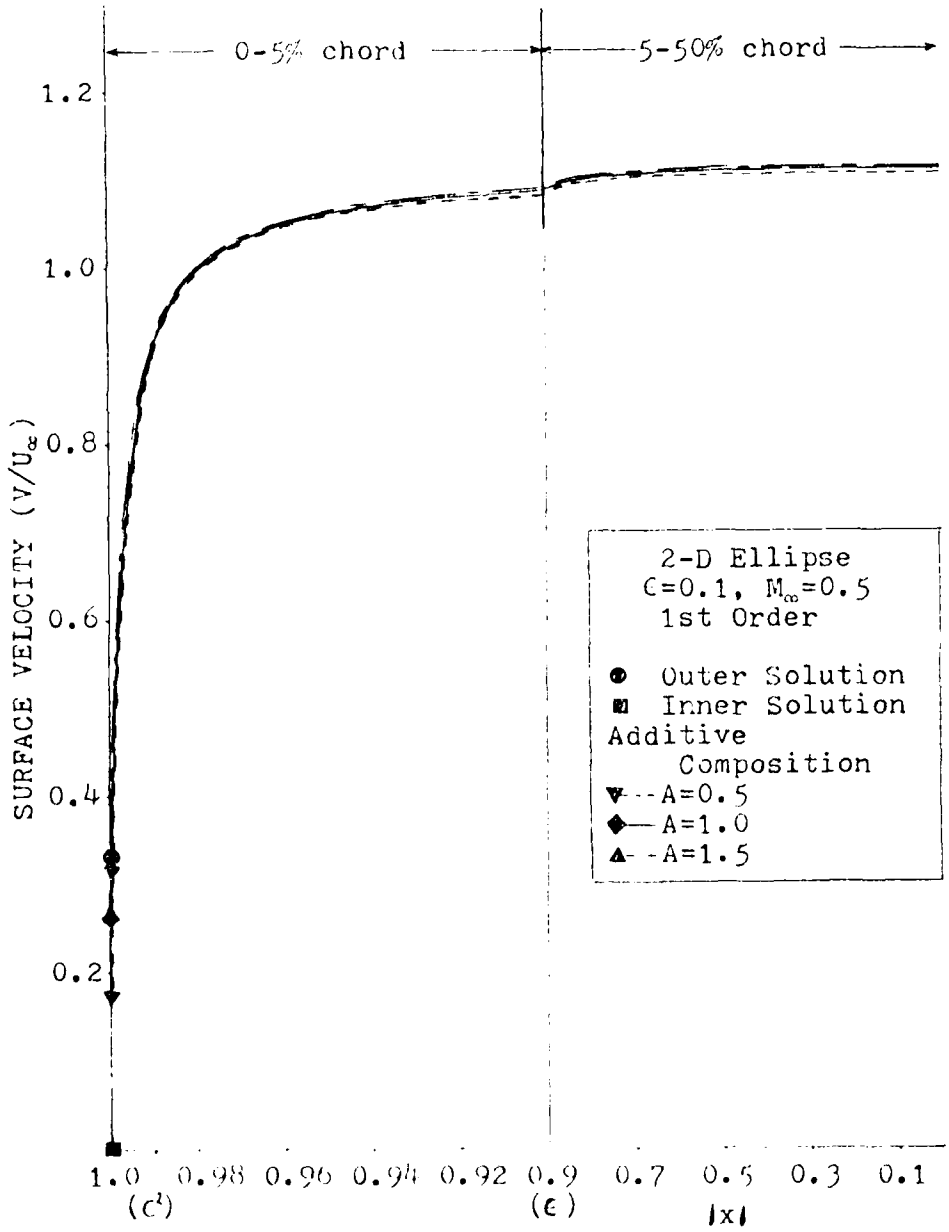

Figure 5. First Order Stagnation Point and Surface Velocity Comparisons, Outer, Inner, and Additive Composite (A=0.5,1.0,1.5) Analytic Solutions, 2-D Ellipse, $\epsilon=0.1$, $M_\infty=0.5$, 0-50% Chord

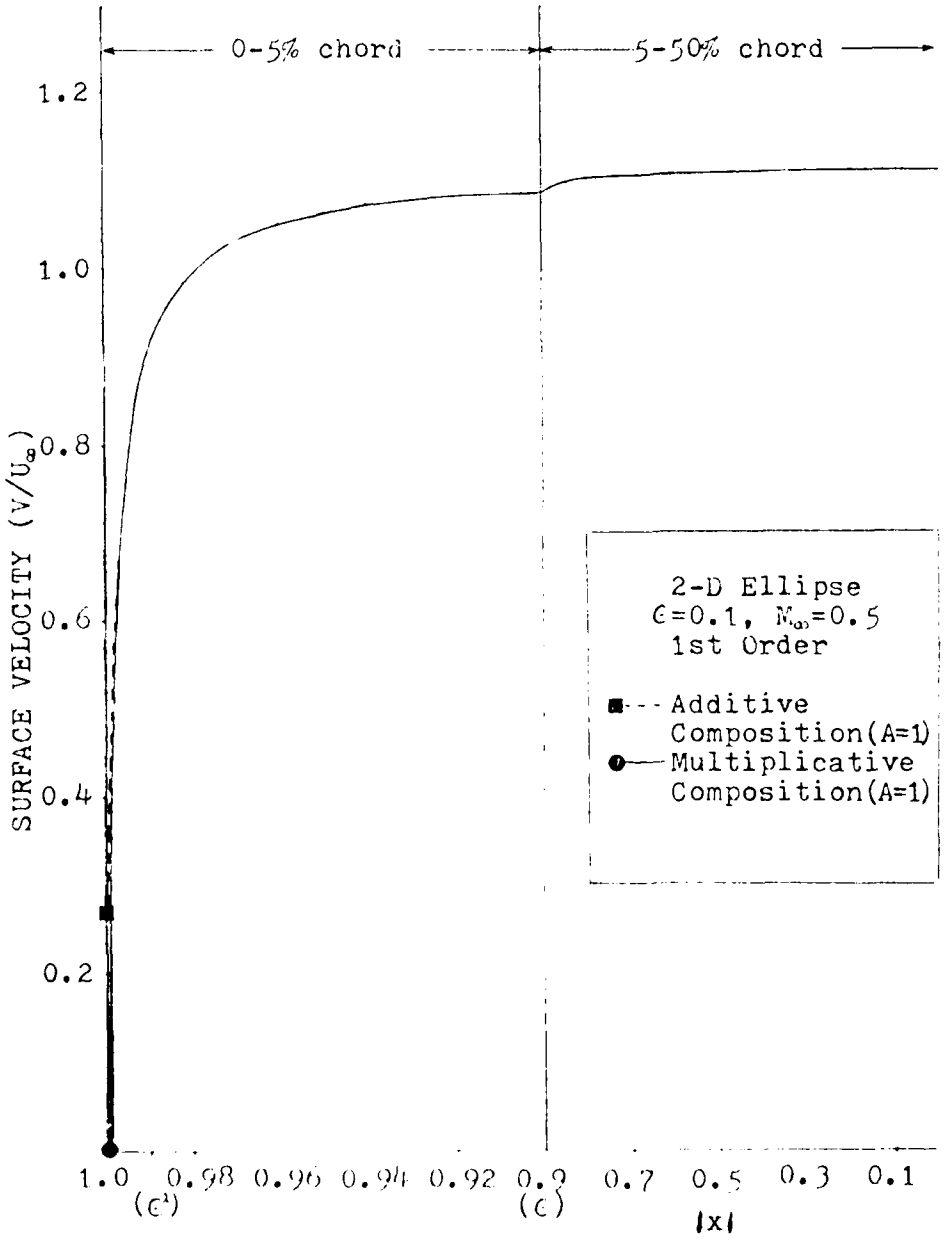

Figure 6. First Order Surface Velocity Comparisons, Additive and Multiplicative Composite Analytic Solutions (A=1), 2-D Ellipse, $\epsilon=0.1$, $M_\infty=0.5$, 0-50% Chord

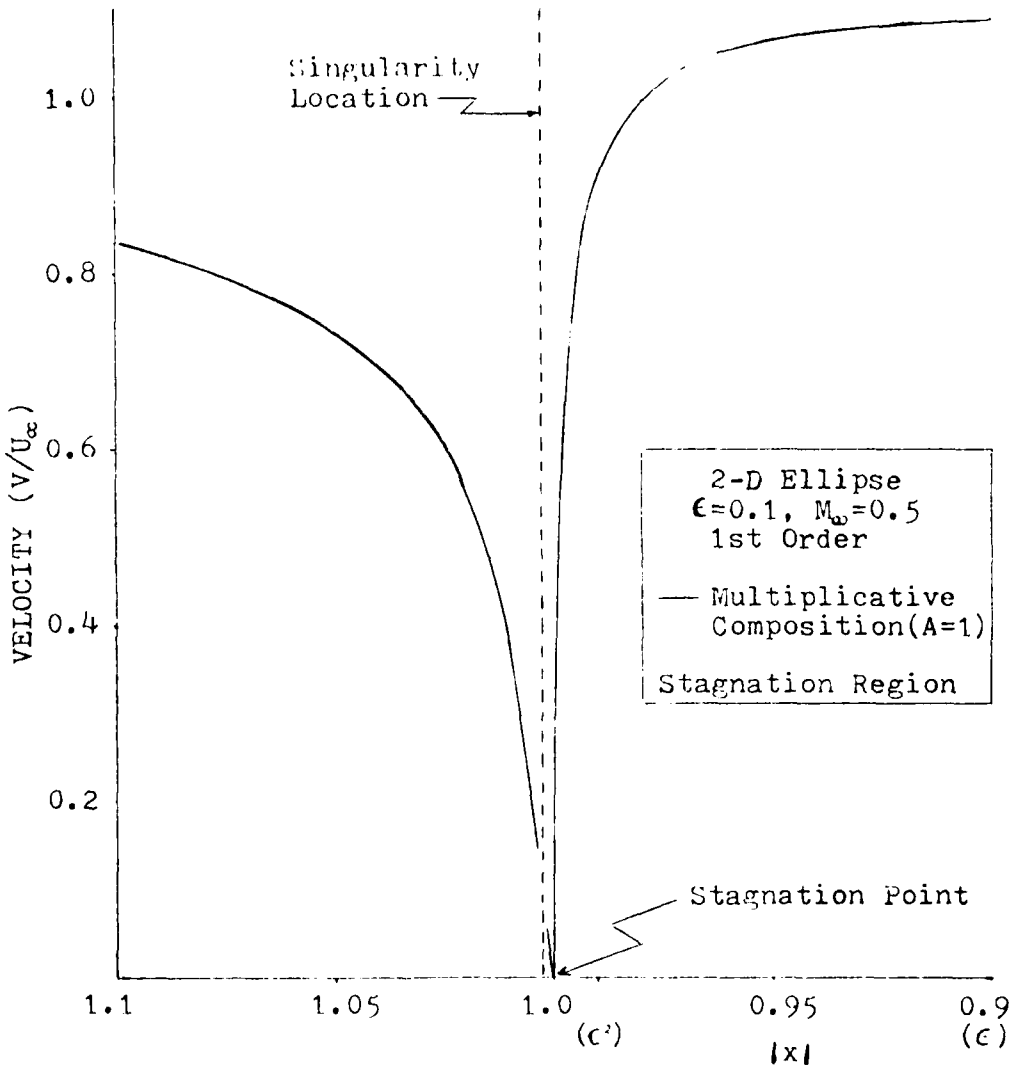

Figure 7. Singular Point Location, First Order Analytic Multiplicative Composite Solution (A=1), 2-D Ellipse, ϵ=0.1, M_∞=0.5

to be preferred to the additive composition. Next, the first order multiplicative composite results will be compared to the results obtained from other methods for a variety of free stream Mach numbers and thicknesses for the ellipse.

Comparison with Other Methods

The best comparison that could be made would be with an exact analytic solution to the full potential equation, Eq (II-9). This is not possible and so the results are compared to numerical solutions obtained from a Jameson code (Ref 16, 17) modeling the full potential equation. The first order multiplicative composite results are also compared with the classic analytic results from thin airfoil theory. The comparisons will be made in terms of the total surface velocity, V/U_∞ (first order composite, Jameson, and thin airfoil theory), and surface perturbation velocity components, u/U_∞ and w/U_∞ (first order composite, Jameson). The comparison will be for ellipses of $\epsilon=0.8$, at $M_\infty=0.1$, $\epsilon=0.5$, at $M_\infty=0.5$, and $\epsilon=0.1$, at $M_\infty=0.1,0.3,0.5,0.6,0.7$, and 0.8. It should be noted that the results from thin airfoil theory represent an asymptotic value in terms of the maximum surface velocity for the first order method (this is consistent with the derivation and the theory).

Figures 8a through 8f (legend for Figs 8a through 8f in Table I) present the surface velocity and perturbation velocity components for the first order multiplicative composition (A=1), exact numerical, and thin airfoil theory solutions. This data is for an elliptic cylinder, $\epsilon=0.1$, at free

stream Mach numbers of 0.1, 0.3, 0.5, 0.6, 0.7, and 0.8. The data at M_∞=0.1 are essentially incompressible while the data at M_∞=0.8 are near the transonic regime. (For most applications M_∞=0.3 is the limit for approximating the flow as incompressible while the transonic flow regime is approximately $0.8 < M_\infty < 1.2$. These of course are only guidelines and depend on the particular configuration.) The first order multiplicative composite solutions are seen to compare very favorably with exact numerical solutions at the lower Mach numbers (M_∞= 0.1, 0.3, and 0.5). As Mach number increases, the agreement, although still very good, begins to decrease until at M_∞=0.8 the composite results are seen to be clearly in error. The discrepancies are due to the dominance of the outer solution in the composite solution. For the maximum velocity, this is primarily due to the fact that as Mach number increases from subsonic to transonic Mach numbers, the assumption that the perturbations remain small becomes less valid. This is clearly shown by the thin airfoil theory solution, being the asymptotic value of the first order composite result. This disagreement between the composite and exact solutions, as Mach number increases, seems to arise primarily in the x-component of the perturbation velocity, u/U_∞, since the agreement in the z-component, w/U_∞, is generally very good for all Mach numbers.

In Figure 8g results are shown for a very thick ellipse, ϵ=0.8, in approximately incompressible flow, M_∞=0.1. These results show that the first order method is good regardless

of thickness for very low Mach numbers. (Again, all solutions are nearly identical for approximately incompressible flows, being exactly identical for $M_\infty=0$.) Finally, in Fig 8h, results are shown for a thick ellipse, $\epsilon=0.5$, at a free stream Mach number of 0.5. As expected the comparison is not good, since the method was developed assuming small perturbations (slender bodies) for the outer solution, that being the dominant solution of the composite. Note however, the inner solution remains quite acceptable.

The results of these comparisons demonstrate that the first order method is a valid approach for obtaining accurate and uniformly valid solutions about slender bodies with round edges in subsonic compressible flow. The first order method is seen to be easily applicable for arbitrary configurations using numerical techniques (Chapter V) that solve the Prandtl-Glauert equation, with the mass flux surface boundary condition. The second order application for the 2-D ellipse is presented in Appendix D while surface values of the term $\beta^2\varphi_{xx}+\varphi_{zz}$ as obtained by various approximations using the first order solutions are presented in Appendix E. The latter comparisons again attest to the validity of the first order method in obtaining uniformly valid solutions as demonstrated in this chapter.

Table I

Legend for Figures 8a-h

2-D Ellipse

— · · —	V/U_∞, Thin Airfoil Theory
	Jameson
o	V/U_∞
□	$\lvert u \rvert / U_\infty$
◇	$\lvert w \rvert / U_\infty$
	1st Order Multiplicative Composition (A=1)
———	V/U_∞
— — —	$\lvert u \rvert / U_\infty$
- - - - -	$\lvert w \rvert / U_\infty$

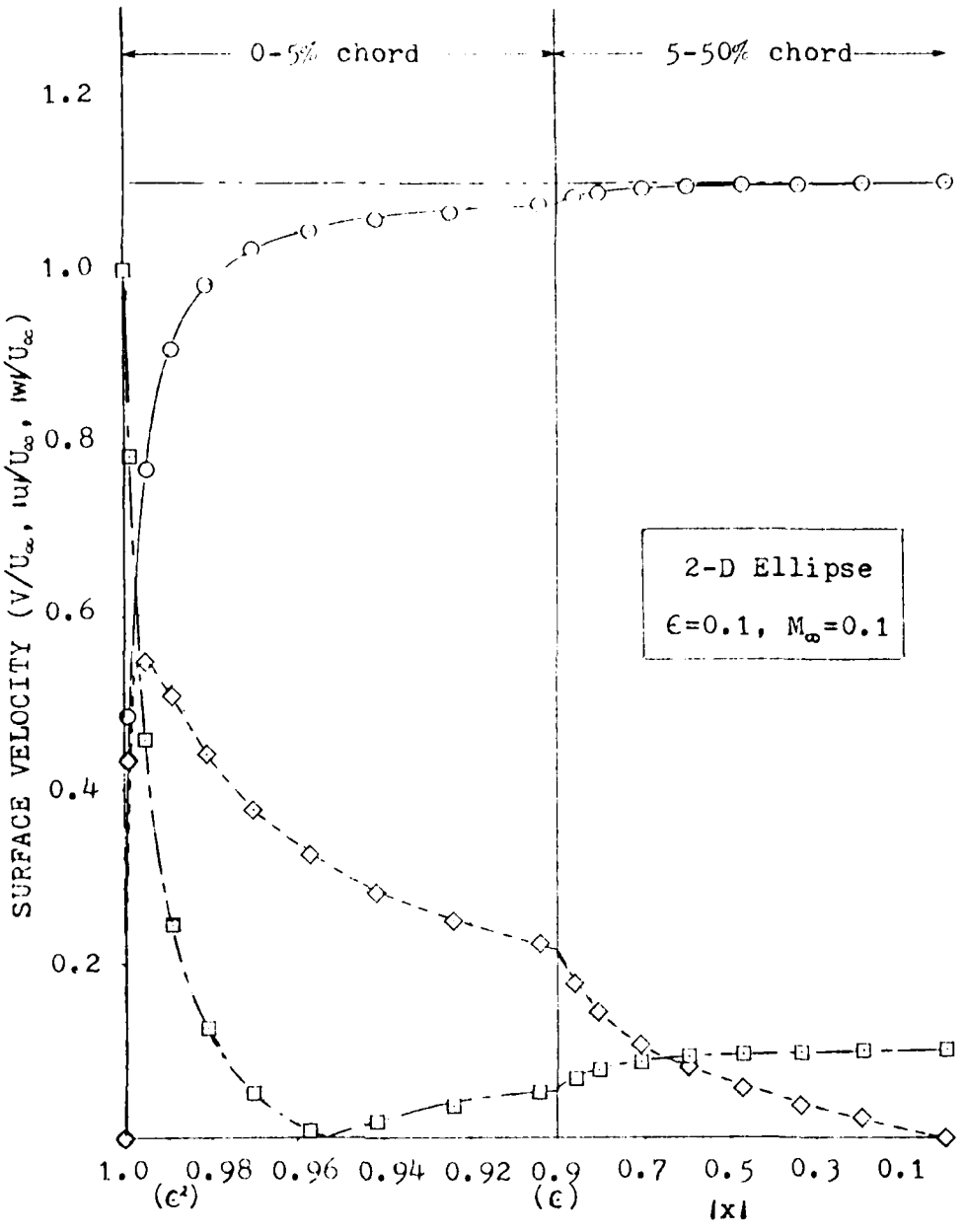

Figure 8a. Total and Perturbation Surface Velocity Comparisons, First Order Analytic Multiplicative Composite (A=1), Thin Airfoil Theory, and Jameson Solutions, 2-D Ellipse, 0-50% Chord, ϵ=0.1, M_∞=0.1

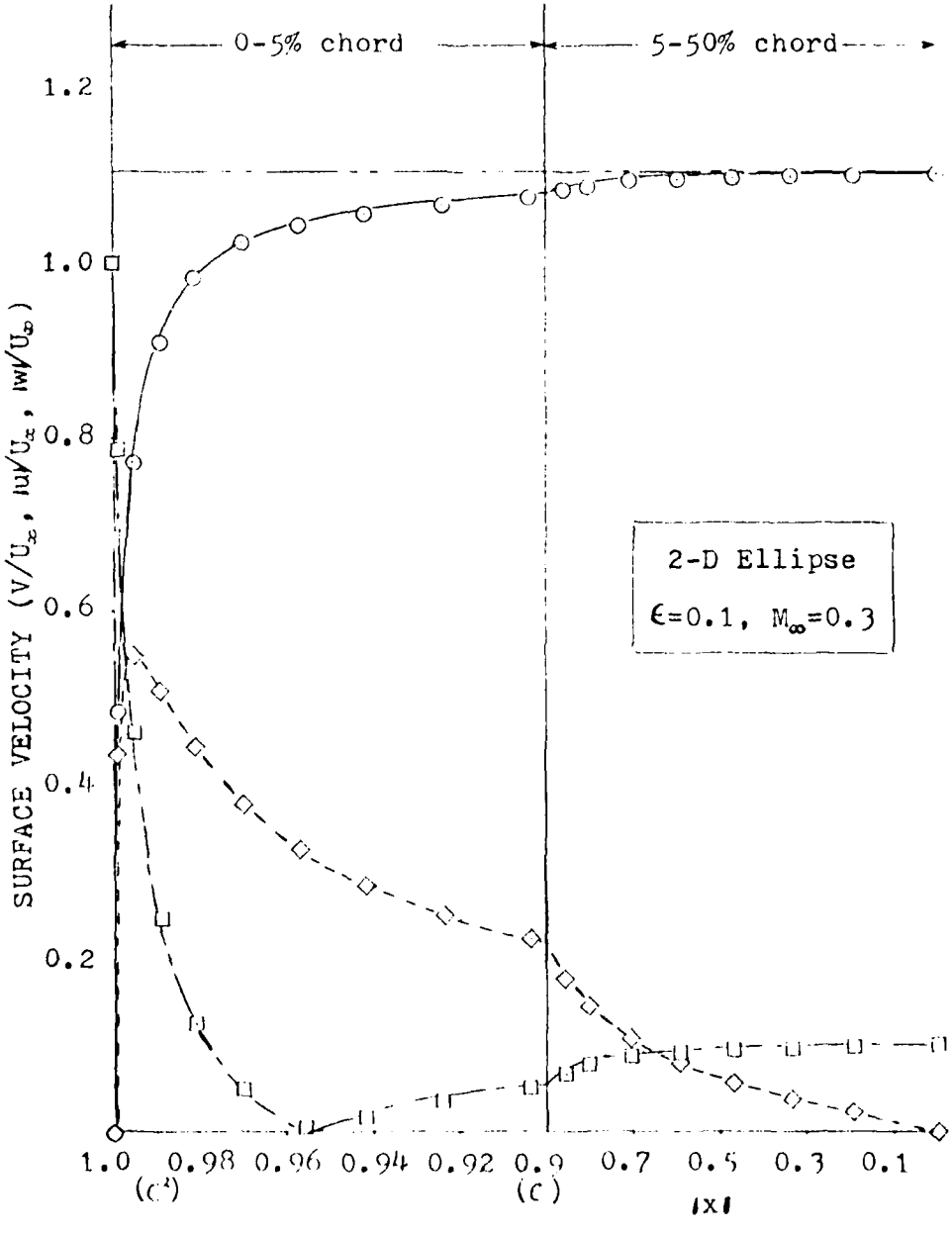

Figure 8b. (continued), $\epsilon=0.1$, $M_\infty=0.3$

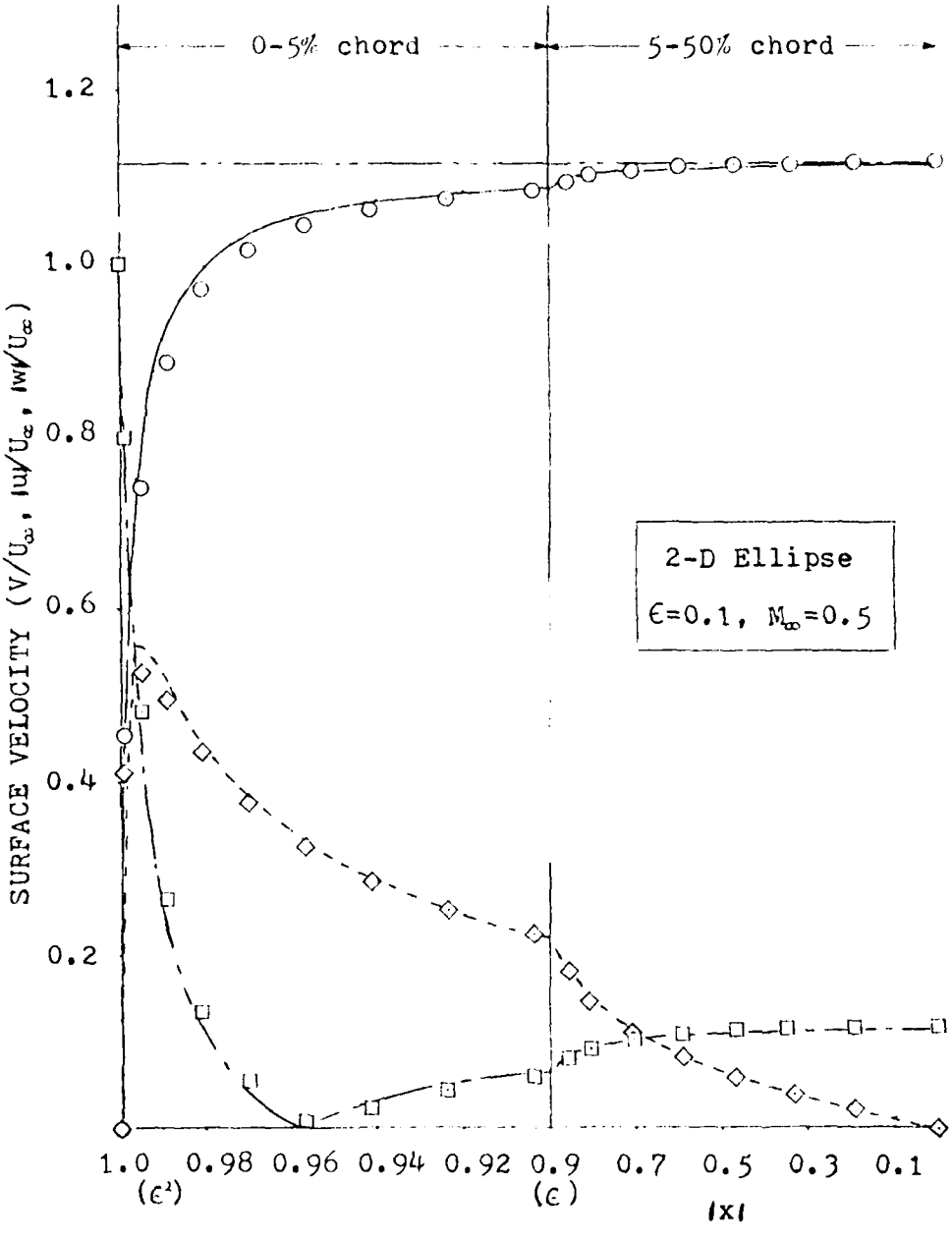

Figure 8c. (continued), $\epsilon=0.1$, $M_\infty=0.5$

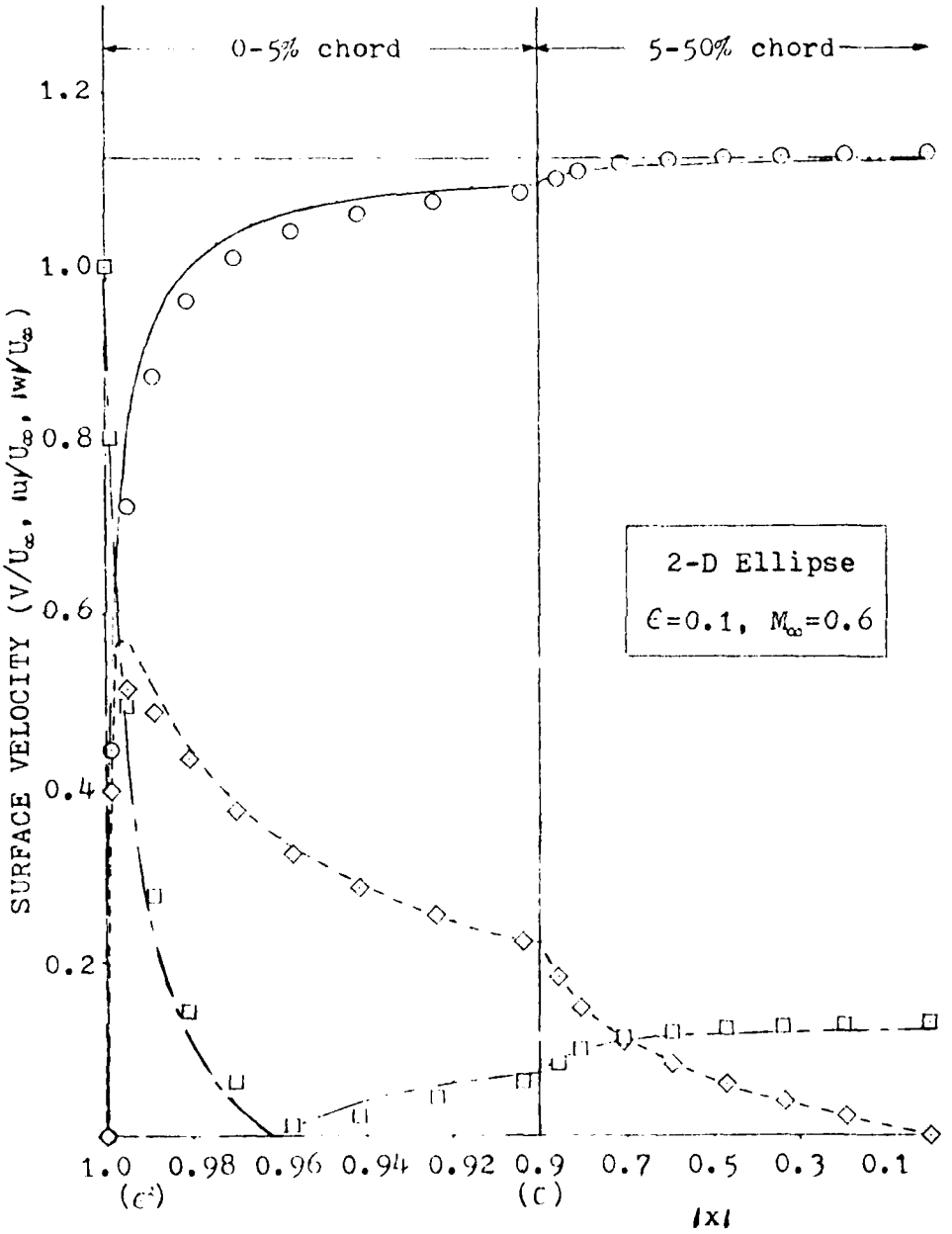

Figure 8d. (continued), $\epsilon=0.1$, $M_\infty=0.6$

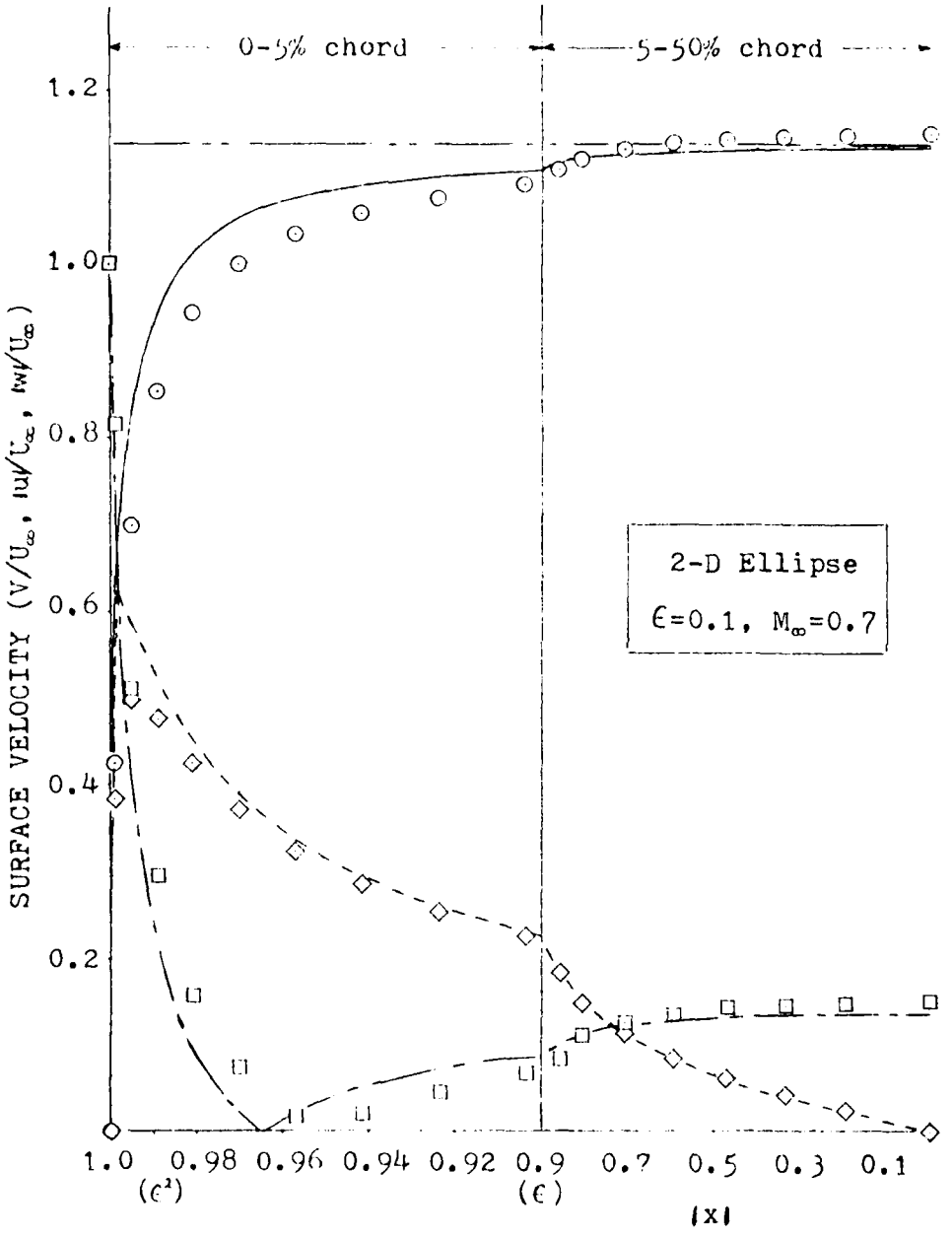

Figure 8e. (continued), $\epsilon=0.1$, $M_\infty=0.7$

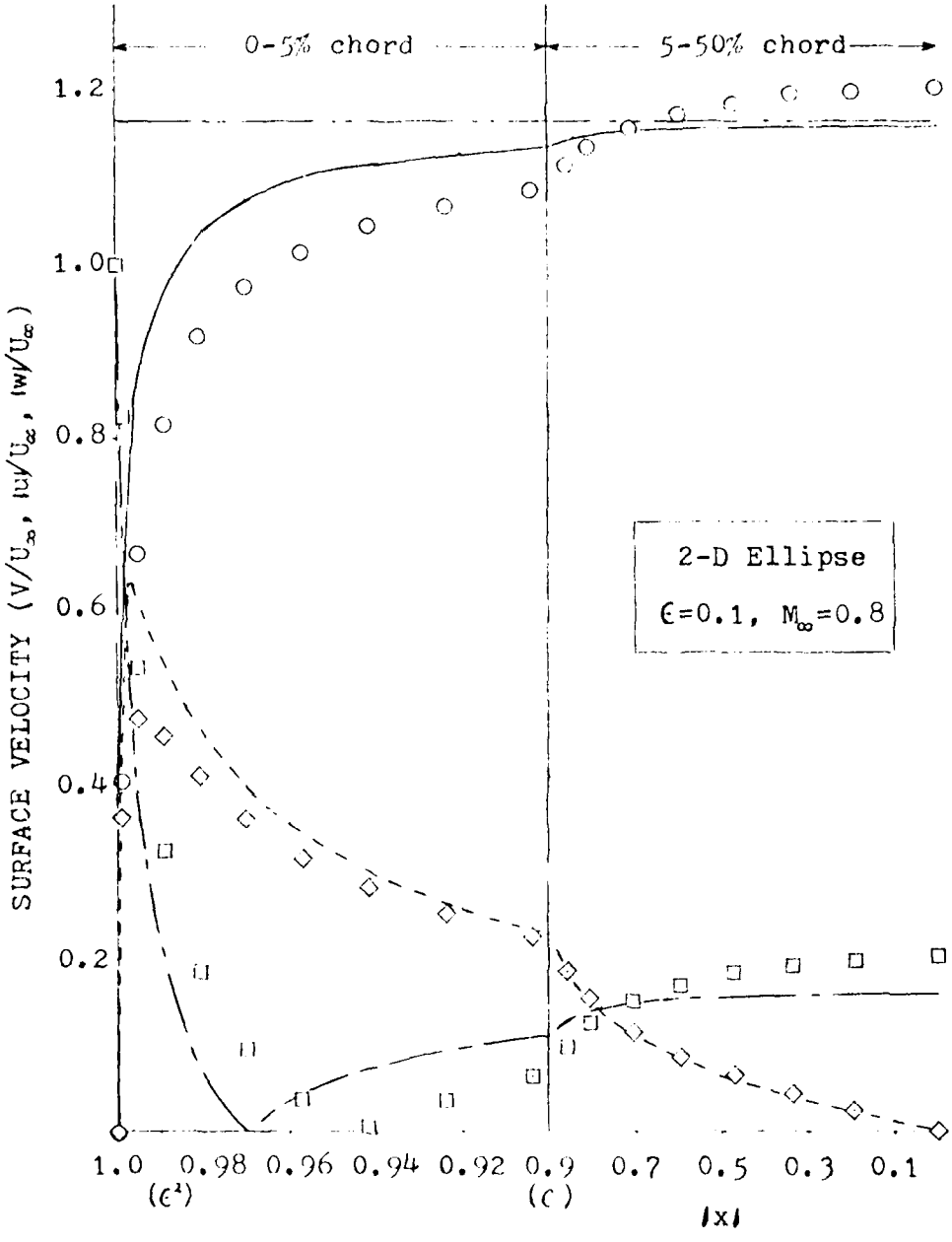

Figure 8f. (continued), $\epsilon=0.1$, $M_\infty=0.8$

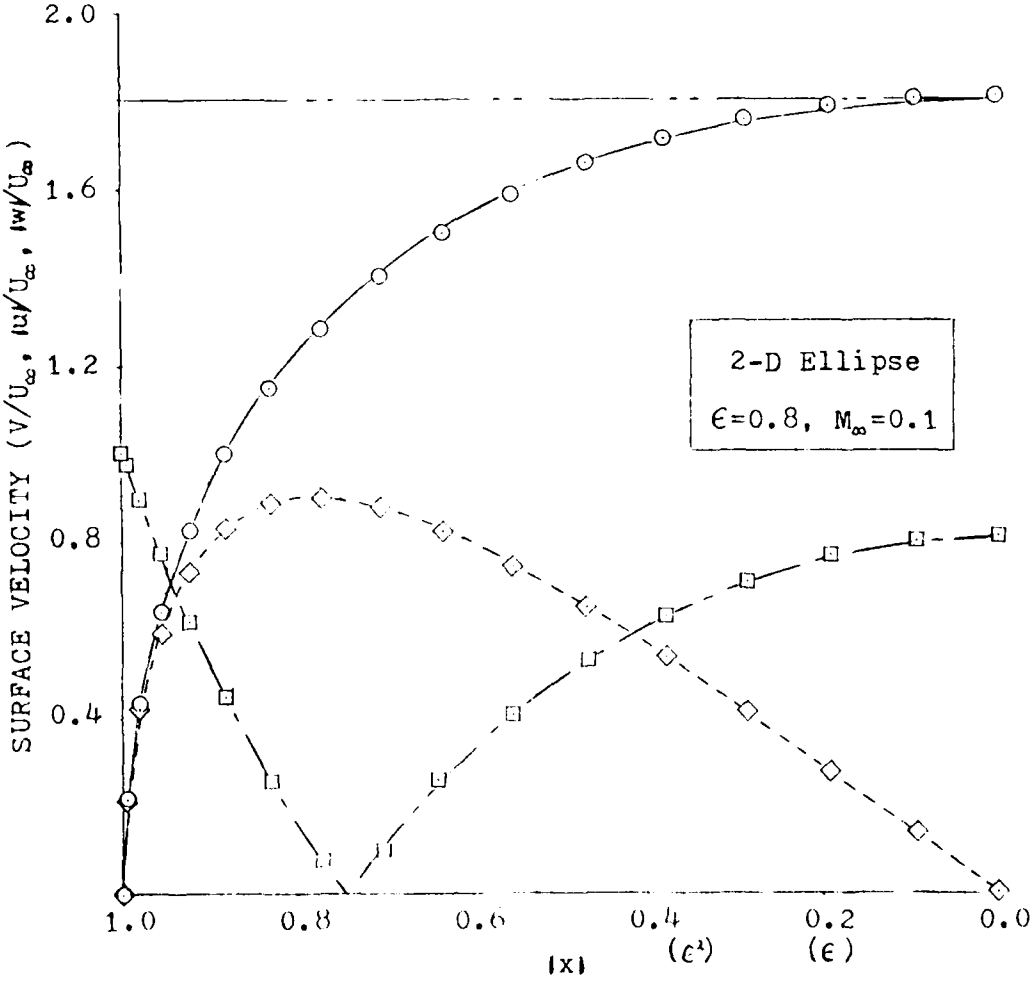

Figure 8g. (continued), $\epsilon=0.8$, $M_\infty=0.1$

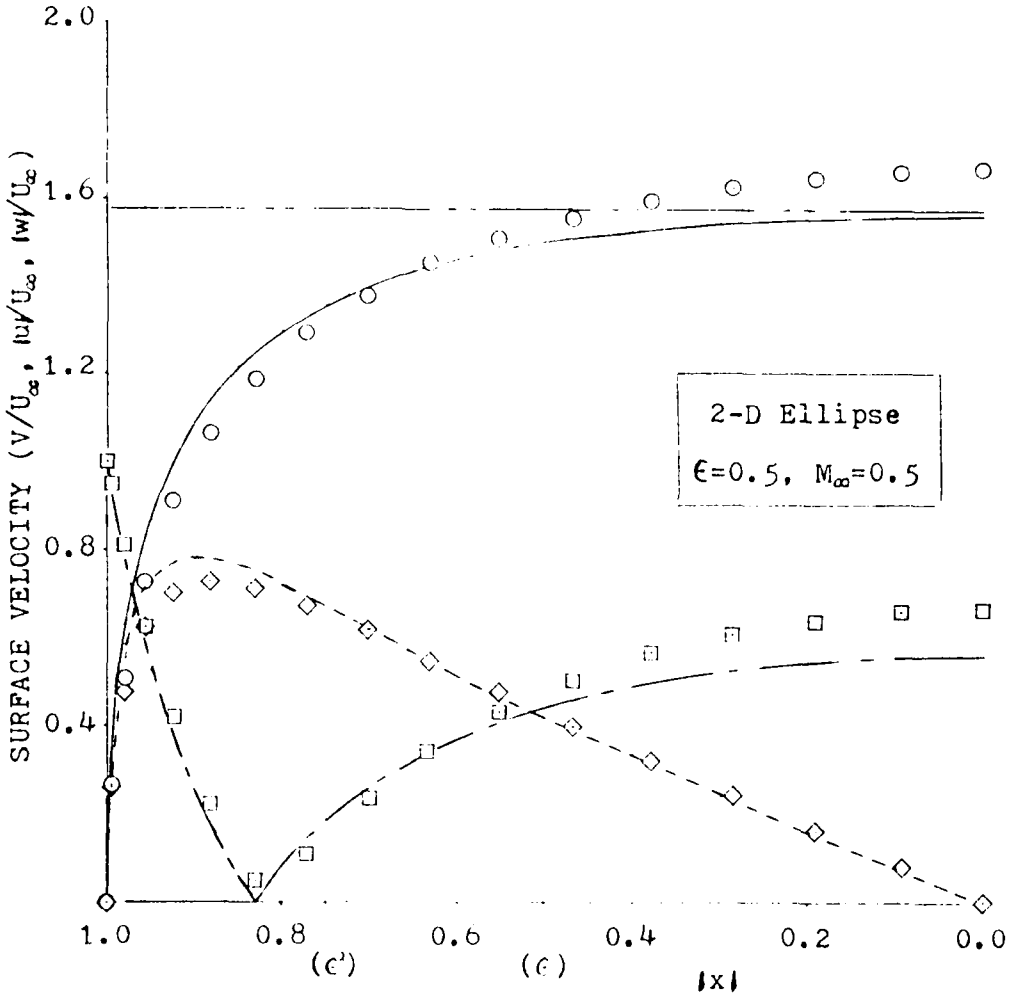

Figure 8h. (continued), $\epsilon = 0.5$, $M_\infty = 0.5$

IV Numerical Application of the First Order Method

The purpose of this chapter is to demonstrate the numerical application of the method by applying the first order method numerically to both 2-D and 3-D bodies in subsonic compressible flow. These results are obtained at zero degrees angle of attack. The numerical technique used was a Woodward code, USSAERO version B (Ref 2), which solves the Prandtl-Glauert equation using distributed surface singularities. Both the velocity surface boundary condition (VBC) and the mass flux surface boundary condition (MFBC) were applied with the latter of course being used to apply the first order method. First, the first order method is applied to a NACA 0012 airfoil and then to a 3-D glide bomb configuration. For the airfoil the first order composite results are compared to the Woodward results (VBC and MFBC), Jameson results, thin airfoil theory (Appendix C), and experimental results (Ref 25, 26). In addition, the Woodward results (VBC and MFBC) will be compared showing the MFBC results to be the better and more correct of the two solutions. For the glide bomb the first order results will be compared only to the Woodward results. In both cases the surface pressures are used to evaluate the inviscid drag coefficients with the result being a constant improvement in value for all Mach numbers using the first order method as compared to the Woodward results. The purpose of this demonstration is to show that the first order method can be easily applied to any numerical

technique that solves the Prandtl-Glauert equation, such as the Woodward code, and that a uniformly valid and more accurate solution results.

Statement of Problem/Method of Solution

The first order governing equation for 2-D problems is

$$B^2\phi_{xx} + \phi_{zz} = 0 \qquad \text{(IV-1)}$$

while for 3-D problems it is

$$B^2\phi_{xx} + \phi_{yy} + \phi_{zz} = 0 \qquad \text{(IV-2)}$$

where as before

$$B^2 = \begin{cases} \beta^2, \text{ outer } (A=0) \\ \Delta, \text{ intermediate } (0<A<2) \\ 1, \text{ inner } (A=2) \end{cases} \qquad \text{(IV-3)}$$

For all applications to follow, A=1, for the intermediate problem. Using the Woodward code, standard results (outer or Prandtl-Glauert equation) are obtained running the configuration at the free stream Mach number. An intermediate solution for the same configuration is obtained for an intermediate Mach number, M_t, given by

$$M_t = \sqrt{1-A} \qquad \text{(IV-4)}$$

for a given value of A. Finally, the inner solution is obtained for the same configuration in incompressible flow, M=0. The first order composite solution is then formed using Eq (II-39) or

$$\frac{V}{U_\infty}\Big|_c = \left(\frac{V}{U_\infty}\Big|_o\right)\left(\frac{V}{U_\infty}\Big|_i\right)\Big/\left(\frac{V}{U_\infty}\Big|_t\right)$$

and the surface pressures (for all solutions) are calculated using the isentropic pressure relationship,

$$C_p = \frac{2}{\gamma M_\infty^2}\left\{\left[1 + \left(\frac{\gamma-1}{2}\right)M_\infty^2\left(1 - \frac{V^2}{U_\infty^2}\right)\right]^{\gamma/\gamma-1} - 1\right\} \qquad \text{(IV-5)}$$

Once the respective solutions have been obtained, the invis-

cid drag coefficients will be evaluated using the surface pressure distributions. For the Woodward code, the accuracy of these calculations of course depends on the number of panels or data points, panel density and distribution. No attempt was made to optimize the panel density and/or distribution for these calculations as only the qualitative comparisons are of interest.

NACA 0012 Airfoil

The first numerical application of the first order method was to a NACA 0012 airfoil (2-D) whose surface is given by (Ref 24),

$$Z_t(x) = \pm 0.6\left\{.2969\sqrt{x} - .126x - .351x^2 + .284x^3 - .102x^4\right\} \qquad \text{(IV-6)}$$

where $Z_t(x)$ is the thickness distribution. The configuration was run using the Woodward code (MFBC and VBC) with the maximum number of chordwise panels (30) at free stream Mach numbers of 0.4, 0.486, 0.6, and 0.71, all at zero angle of attack.

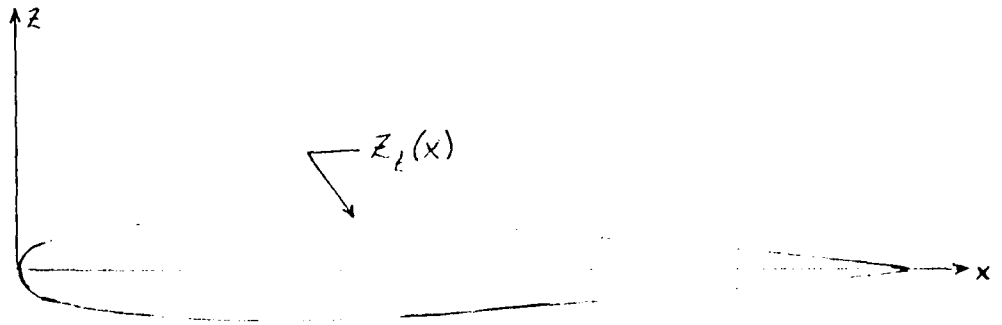

Figure 9. NACA 0012 Airfoil

The MFBC Woodward solutions form the outer or Prandtl-Glauert solution used in the formation of the composite solution. The same configuration was then run (MFBC) at intermediate Mach numbers of 0.198, 0.239, 0.292, and 0.342 for the intermediate solution (A=1), and then finally at M=0 for the inner solution. The solutions were then combined to form uniformly valid solutions using the multiplicative composition, Eq (II-40), in terms of the surface velocity. Results were compared to the Jameson code, analytic thin airfoil theory (Appendix C) as well as experimental data.

Results of the numerical application of the first order method are shown in Figs 10a through 10d. Shown are the surface pressure distributions (C_p) for the free stream Mach numbers of 0.4, 0.486, 0.6, and 0.71. At each Mach number the composite results are compared to the VBC and MFBC Woodward results, Jameson, thin airfoil theory, and experimental free flight or wind tunnel data (Ref 25,26). For all the Mach numbers, the thin airfoil theory results are clearly in error in the stagnation region. However, these results are a reasonable approximation to the adverse pressure gradient. The Jameson or exact numerical solution, as compared to the Woodward (VBC and MFBC) and composite solutions, is seen to have higher negative peak pressures near the point of maximum surface velocity which becomes more apparent as Mach number increases. In comparing the two Woodward solutions it is readily seen as Mach number increases that the MFBC solution is the better solution with respect to the Jameson re-

sults. Both solutions yield approximately the same maximum surface velocity but the MFBC solution is a better match to the Jameson solution in the stagnation region. This difference in the stagnation region will show up dramatically in the inviscid drag calculations. The first order composite solutions, being formed using the MFBC Woodward solutions, are also a very good match in the stagnation region to the Jameson solution, especially since they are identical at the stagnation point. The ability to correctly model the flow in the stagnation region, as previously pointed out, is important as the results of the inviscid drag calculations will demonstrate. One limitation of the first order method and Woodward solutions is clearly shown in Fig 10d in the inability to accurately predict the maximum surface velocity (Jameson solution) as the flow approaches the transonic regime. As previously noted these first order methods are only valid for subsonic or supersonic flows. The experimental data is matched well by all solutions except at the trailing edge in Figs 10b and 10d where the viscous effects become apparent, and only the Jameson solution is a good match to this data as the flow approaches transonic Mach numbers (Fig 10d). These comparisons verify the fact that inviscid methods are able to accurately model real flow behavior when used prudently.

The resultant inviscid drag coefficients per unit span were determined using the pressure distributions shown in Figs 10a through 10d, the theoretical value of course being

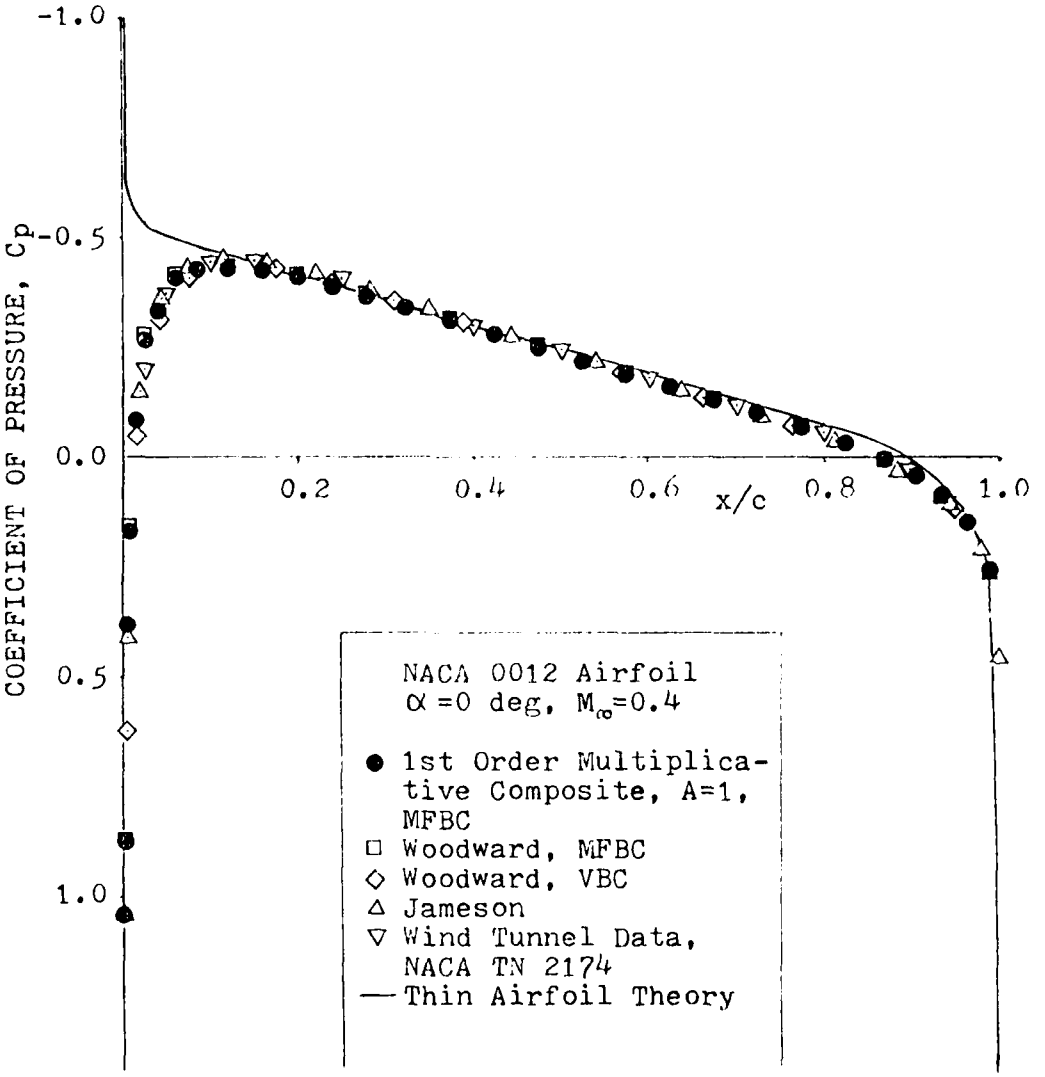

Figure 10a. Comparison of Surface Pressure Distributions, First Order Multiplicative Composite (A=1), Woodward (VBC and MFBC), Jameson, Thin Airfoil Theory Solutions, and Experimental Data, NACA 0012 Airfoil, α=0 deg, M_∞=0.4

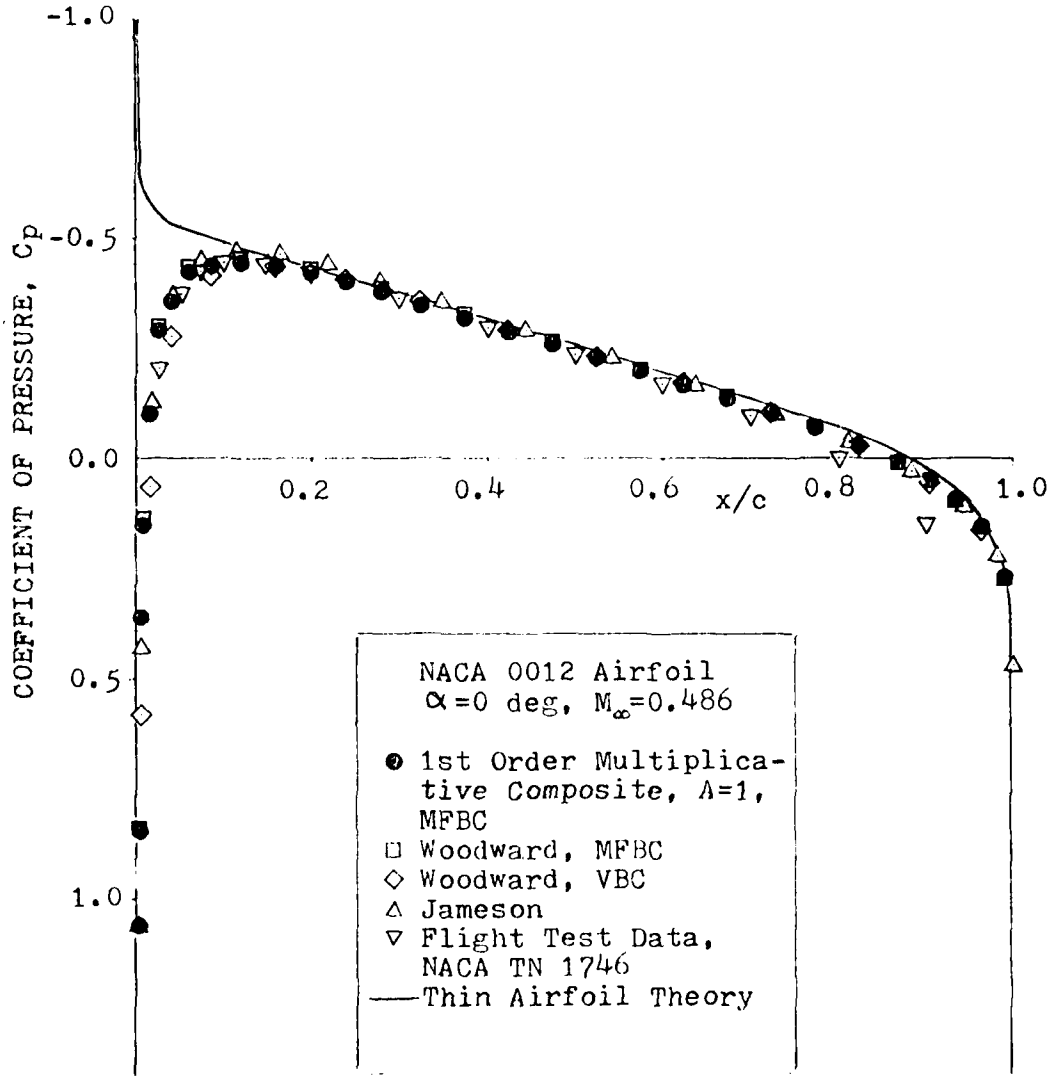

Figure 10b. (continued), M_∞=0.486

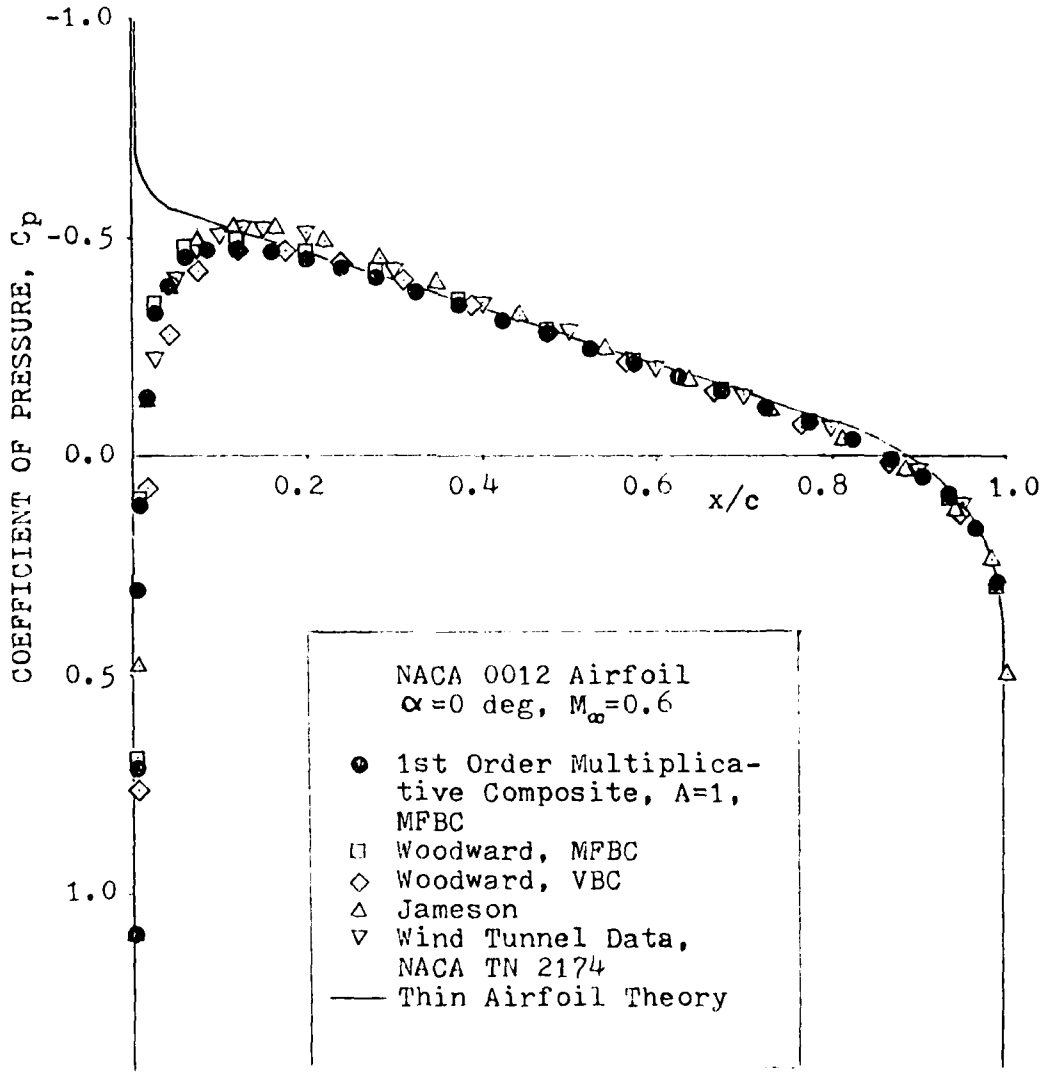

Figure 10c. (continued), M_∞=0.6

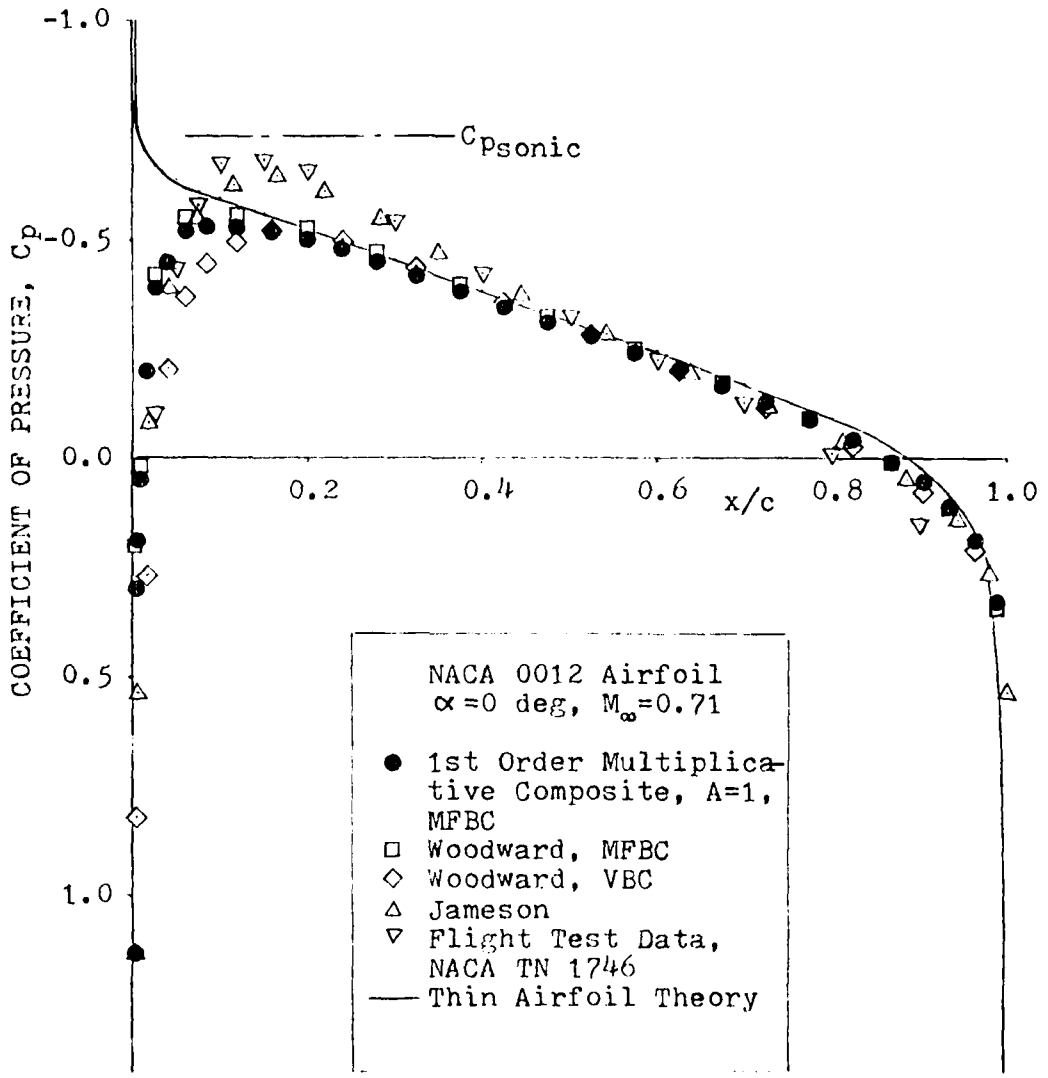

Figure 10d. (continued), M =0.71

Table II

Comparison of Drag Coefficients per unit span
NACA 0012 Airfoil

	M_∞ 0.4	0.486	0.6	0.71
Jameson	-.000062	-.000077	-.000109	-.000162
Woodward, VBC	.00515	.00691	.01136	.01656
Woodward, MFBC C_{d_w}	-.00227	-.00468	-.01103	-.02550
1st Order (A=1) Composite, MFBC C_{d_c}	-.00005	-.00158	-.00555	-.01408
$\Delta C_d = \lvert C_{d_w} - C_{d_c} \rvert$	.00222	.00310	.00548	.01142
% Reduction, $\Delta C_d / C_{d_w}$	97.8	66.2	49.6	44.7

zero for 2-D inviscid flow. These results are shown in Table II as computed for the Jameson, Woodward (VBC and MFBC), and composite solutions, where

$$C_d = D' / \tfrac{1}{2} \rho_\infty U_\infty^2 c \qquad \text{(IV-7)}$$

and

$D' \triangleq$ Drag per unit span (lb_f/ft)

The surprising thing to note in Table II is the level of the inviscid drag coefficients for the Woodward results in light of the theoretical result being zero. With these levels it is easily understood why difficulties are encountered in estimating inviscid drag levels for 3-D configurations (drag due to lift). Regardless, it is seen that this effort can be appreciably aided by using the uniformly valid composite solution. Although the differences in pressures (Figs 10a

through 10d) between the Woodward and composite solutions appear negligible, there is a consistent reduction in the drag coefficients for all Mach numbers. This reduction, in the direction of the exact solution, is directly due to the correction made in the stagnation region, thus the direct benefit of using a uniformly valid composite solution has been demonstrated. Being able to better predict inviscid drag levels for initial performance estimates (including viscous drag) and using uniformly valid pressure distributions only enhances the design process.

Before leaving this table it is interesting to note that when the VBC is applied using the Woodward code, positive values of C_d result while when using the MFBC negative values of C_d result. Recall that in Chapter I it was stated that when using thin airfoil theory results to calculate the inviscid drag of a nonlifting body in compressible flow, it becomes necessary to add a leading edge drag term to obtain the correct inviscid result of zero. In other words the thin airfoil theory solution itself results in a thrusting body which is consistent with the results obtained using the Woodward code with the MFBC. This again leads one to believe that that the MFBC is the correct equation to be used for these approximations.

Glide Bomb

The final application of the first order method is to the 3-D glide bomb configuration (Ref 27) shown in Fig 11. This configuration (originally a proposed submunition) is

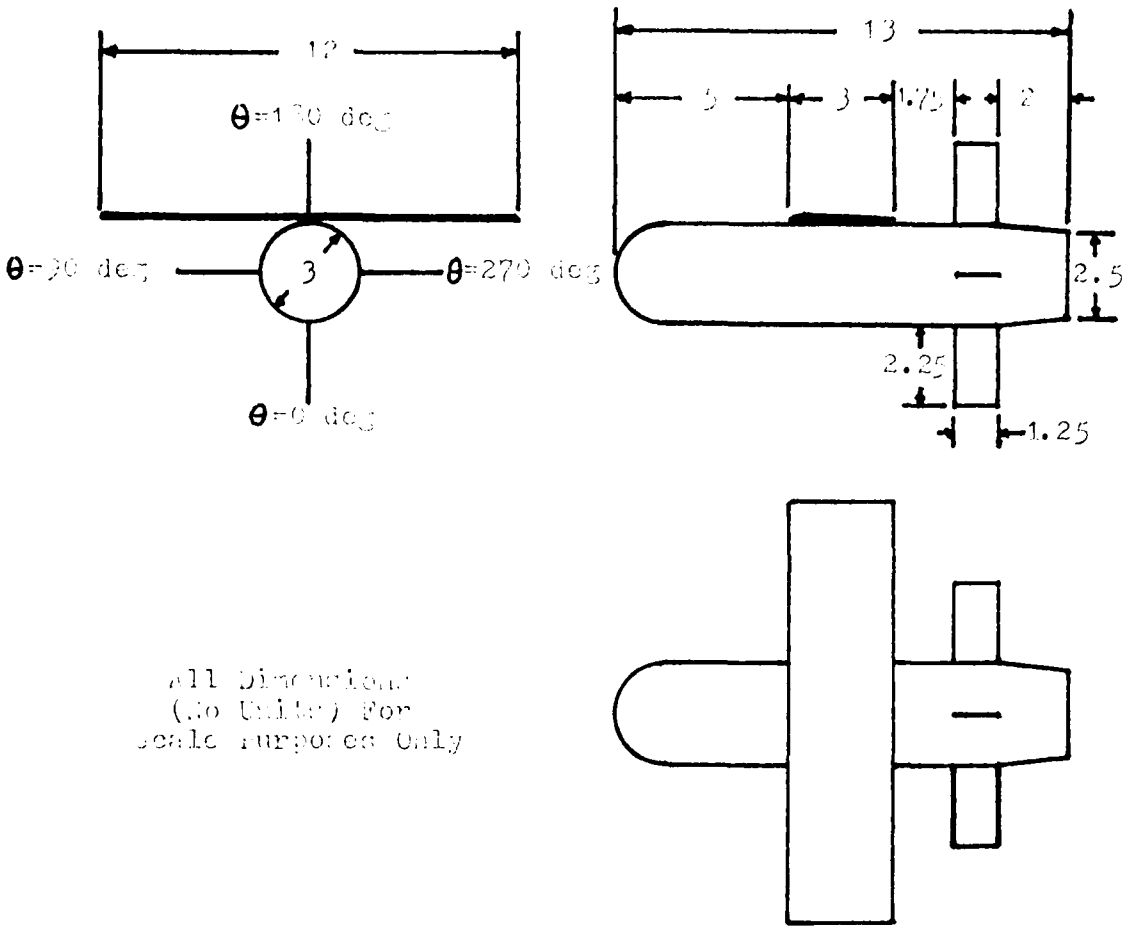

Figure 11. Glide Bomb

typical of the current glide bomb (and cruise missile) configurations that operate in the subsonic speed range. It has a hemispherical nose with a cylindrical body and aft boattail. The planar wing, in this case with NACA 0012 airfoil sections, is mounted on the top of the body. The cruciform tail consists of four flat plates with round leading edges. The configuration was run at a zero angle of attack using the Woodward code (MFBC) at free stream Mach numbers of 0.3, 0.4, 0.5, and 0.6. The corresponding intermediate solutions (A=1) were obtained at intermediate Mach numbers of 0.149, 0.198, 0.245, and 0.292. The inner solution was again obtained for the incompressible flow case, M=0. Surface pressure data are presented in Figures 12 and 13 for the Woodward and first order multiplicative composite solutions for the free stream Mach number of 0.5. These data are representative of the data at the other Mach numbers. In Fig 12 is presented the body surface pressures and Fig 13 presents the wing upper and lower surface pressures. The total number of body panels used was 180 and the total number of wing and tail panels used was 96. No attempt was made to increase panel density to improve the results as would occur in the design process.

The body surface pressures shown in Fig 12 are at various meridan angles about the body. There is very little difference in the results except in the stagnation regions (both the nose of the body and near the wing leading edge), as before with the NACA 0012 airfoil data. The same is true of the wing surface pressure data as shown in Fig 13 for three

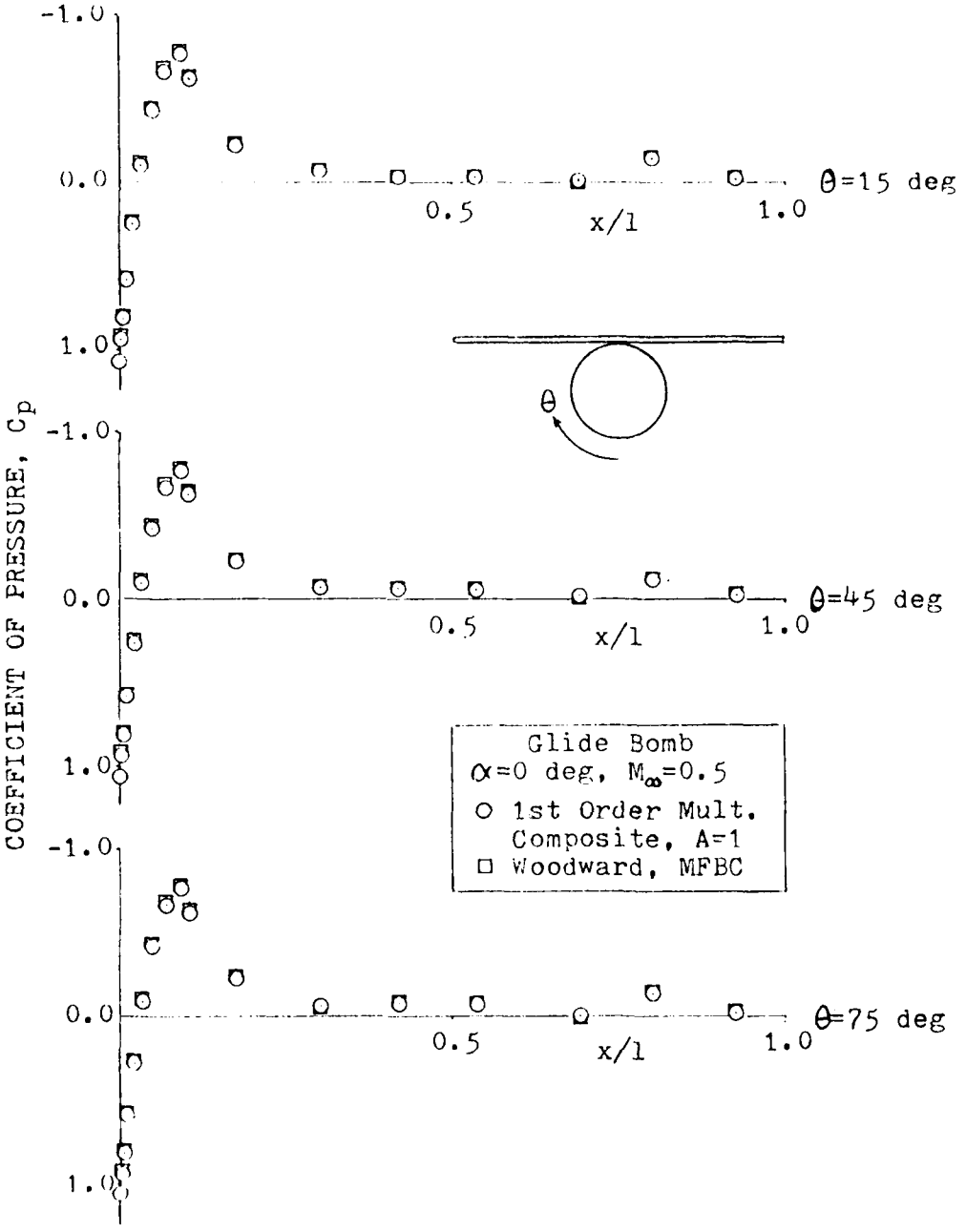

Figure 12. Comparison of Body Surface Pressure Distributions, First Order Multiplicative Composite (A=1) and Woodward (MFBC) Solutions, Glide Bomb, α=0 deg, M_∞=0.5

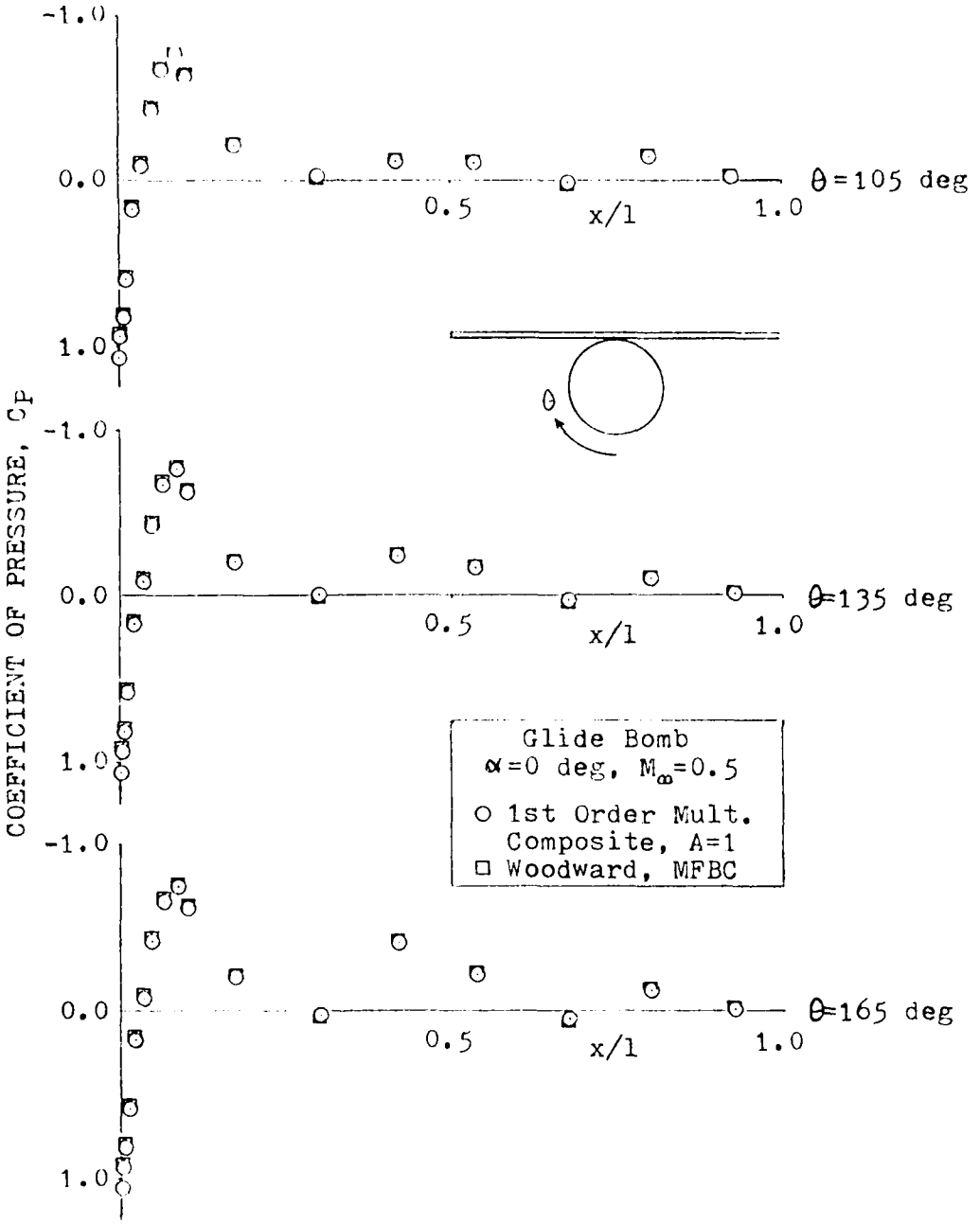

Figure 12. (continued)

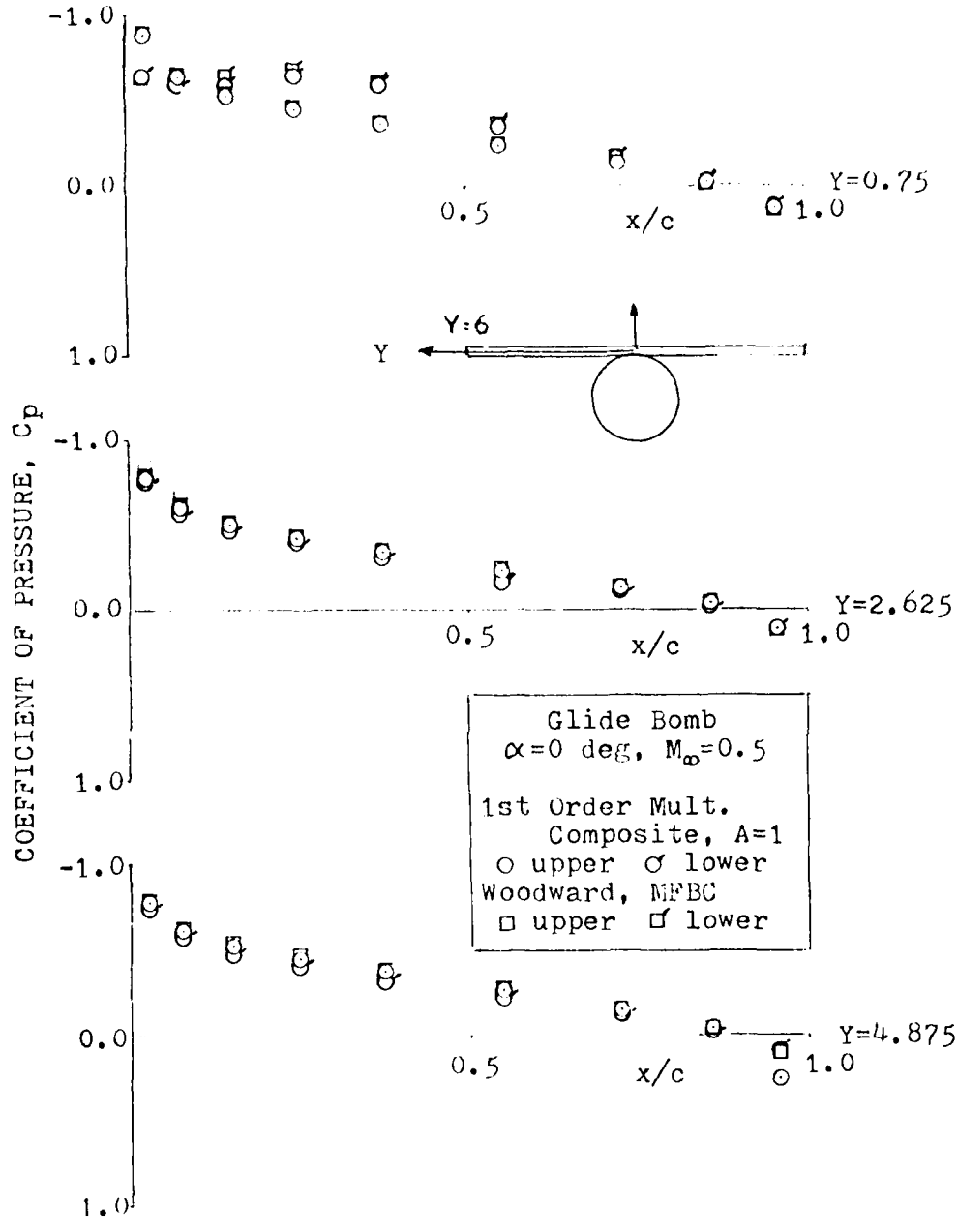

Figure 13. Comparison of Wing Upper and Lower Surface Pressure Distributions, First Order Multiplicative Composite (A=1) and Woodward (MFBC) Solutions, Glide Bomb, α=0 deg, M_∞=0.5

spanwise stations on the right wing. For the body data the same trends are observed as before for the flow about the nose or stagnation region. The composite results show a slightly higher velocity in this region and reduced negative peak pressures as compared to the Woodward results. For the wing data, Fig 13, the velocities in the stagnation region for the composite solution are again slightly higher than the Woodward results, however, the inboard station shows a slightly greater negative peak pressure while the outboard station is slightly less than the Woodward results. One can clearly see in Fig 12 the ever increasing presence of the wing as one moves around the body, while in Fig 13 the outboard loading is somewhat less than the inboard due to the presence of the wing tip.

The resultant drag coefficients were calculated using the surface pressure data where

$$C_D = D/\tfrac{1}{2}\rho_\infty U_\infty^2 S \qquad \text{(IV-8)}$$

and

$$D \triangleq \text{Pressure or Form Drag } (lb_f)$$

with the results being presented in Table III. Although the configuration was at a zero angle of attack a negligible lift was produced due to the high mounted wing and resulting wing body interference. As shown in Table III there is again a consistent reduction in the value of the drag coefficients even though the difference in pressure distributions was again slight. This is directly the result of using a solution (composite) which more accurately models the flow in stagna-

Table III

Comparison of Drag Coefficients
Glide Bomb Configuration

	M_∞ 0.3	0.4	0.5	0.6
Woodward, MFBC C_{D_W}	-.06822	-.07026	-.07449	-.08364
1st Order (A=1) Composite, MFBC C_{D_C}	-.06736	-.06869	-.07252	-.07917
$\lvert\Delta C_D\rvert$, Drag Counts	8.6	15.7	19.7	44.7

tion regions. Although the difference in pressure distributions is slight, these differences are important for drag calculations. Note again the relatively high values for the inviscid drag coefficients in light of the theoretical value being zero for nonlifting bodies. The results show the first order method to be an easily applicable and accurate method for obtaining uniformly valid solutions about 2-D and 3-D configurations with round leading/trailing edges in subsonic potential flow. The proposed method has also been demonstrated to be easily applicable to a current numerical technique solving the Prandtl-Glauert equation. Application of the proposed method has resulted in consistently improved inviscid drag estimates. Although the results presented have been for nonlifting bodies only, the first order method can be easily extended to lifting problems (camber and or angle of attack), however this remains to be verified.

V Conclusions

The purpose of this dissertation was to develop a method, based on the principles of singular perturbation theory, for obtaining uniformly valid solutions about slender bodies with round leading/trailing edges in subsonic potential flow. The first order method as developed using the multiplicative composition has been shown to satisfy this goal. Specifically:

1. The first order method corrects small perturbation theory (outer or Prandtl-Glauert solution) with a stagnation region theory (inner solution) yielding uniformly valid solutions. The method was developed by formulating approximate equations to the exact potential equation, and mass flux surface and infinity boundary conditions. The mass flux surface boundary condition was shown to be the boundary condition to use for these approximations.

2. Analytic solutions were developed for application of the first order method to the 2-D ellipse with the results being compared with thin airfoil theory and a numerical solution of the exact potential equation as developed by Jameson. Comparisons with the Jameson results were very favorable within the limitations of the theory, that is for slender bodies in subsonic compressible flow.

3. The first order method was then applied numerically, using a panel method as developed by Woodward, to a NACA 0012 airfoil with the results being compared again to Jameson results, Woodward results, thin airfoil theory, and experimental data. The comparisons again proved to be very favorable within the

limitations of the theory. Next, the first order method was applied numerically to a 3-D glide bomb configuration using the Woodward code with the results being compared to the Woodward or outer solution results. The numerical applications of the first order method demonstrated the ease of applicability and the versatility of this proposed method for any numerical technique solving the Prandtl-Glauert equation with the appropriate boundary conditions.

4. The latter two numerical applications of the first order method resulted in consistent improvements in the prediction of inviscid drag levels as compared to the Woodward results. This increase in accuracy leads directly to increased confidence in inviscid aerodynamic predictions and their later use when predicting viscous effects. This increase in accuracy has been shown to be directly due to the correction made to the outer solution in the stagnation region by using the composite solution.

5. Finally, and most importantly, the method as proposed obviates the need for analytic solutions or numerical patching of solutions in forming a uniformly valid composite solution. Three solutions are required for the composite solution. all being solutions to the Prandtl-Glauert equation for the same surface at three different Mach numbers (M_∞, M_1, and M=0). The composite solution once obtained offers increased accuracy of simulation as demonstrated in this effort.

Before closing one item should be remembered in light of the results. This concerns the perturbation parameter, ϵ, which was assumed to be small throughout this effort. Small

is a relative term, however, usual definitions (Ref 7,19) imply that the perturbation parameter is on the order of ten percent (or less) of the parameter being perturbed. For practical application, however, an upper limit of fifteen percent is often used. Applications beyond these limits are at the expense of reduced accuracy. All applications of the proposed method in this effort have been for thickness ratios of ten percent or greater and thus the method has been tested for the extreme cases in terms of the perturbation parameter and accuracy. For application of the method to thinner bodies the results should be even better.

To summarize then, the first order method is a highly accurate and easily applicable technique for obtaining uniformly valid results about slender bodies with round leading/trailing edges in compressible subsonic potential flow. The method as developed was applied to nonlifting bodies only, however, the method can and should be developed for lifting bodies (camber and or angle of attack).

Bibliography

1. Woodward,F.A. "Analysis and Design of Wing-Body Combinations at Subsonic and Supersonic Speeds," J.Aircraft, Vol 5, No 6: 528-534 (Nov-Dec 1968).

2. Woodward,F.A. "An Improved Method for the Aerodynamic Analysis of Wing-Body-Tail Configurations in Subsonic and Supersonic Flow." NASA CR-2228, Part I. 1973.

3. Hess,J.L. and Smith,A.M.O. "Calculation of Potential Flow about Arbitrary Bodies," Progress in Aeronautical Science, Vol 8. 1-138. New York: Pergamon Press, 1966.

4. Hess,J.L. "The Problem of Three-Dimensional Lifting Potential Flow and its Solution by means of Surface Singularity Distribution," Computer Methods in Applied Mechanics and Engineering, Vol 4. 1974.

5. Ehlers,F.E., Johnson,F.T., and Ruppert,P.E. "Advanced Panel-Type Influence Coefficeint Methods Applied to Subsonic and Supersonic Flows," Aerodynamic Analysis Requiring Advanced Computers, NASA SP-347, Part II. 939-984. 1975.

6. Morino,L. "A General Theory of Unsteady Compressible Potential Aerodynamics," NASA CR-2464. 1974.

7. Liepmann,H.W. and Roshko,A. Elements of Gasdynamics (Sixth Edition). 202-206. New York: John Wiley and Sons, Inc., 1965.

8. Stancil,R.T. "Improved Wave Drag Predictions Using Modified Linear Theory," J.Aircraft, Vol 16, No 1: 41-46 (Jan 1979).

9. Olsen,J.J. Subsonic and Transonic Flow Over Sharp and Round Nosed Nonlifting Airfoils. Ph.D. Thesis. Ohio: The Ohio State University, 1976.

10. Lighthill,M.J. "A New Approach to Thin Airfoil Theory," Aero. Quart., 3: 193-210 (1951)

11. Van Dyke,M. "Second-Order Subsonic Airfoil Theory Including Edge Effects," NACA Rpt 1274. 1956.

12. Jones,R.T. "Leading-Edge Singularities in Thin-Airfoil Theory," J.Aero. Sci., 17: 307-310 (May 1950).

13. Heaslet,M.A. and Lomax,H. "Supersonic and Transonic Small Perturbation Theory," General Theory of High Speed Aerodynamics, Vol 6, High Speed Aerodynamics and Jet Propulsion, edited by W.R. Sears. 143-148. Princeton, New Jersey: Princeton University Press, 1954.

14. Sotomayer,W.A. and Weeks,T.M. "Aerodynamic Analysis of Supersonic Aircraft with Subsonic Leading Edges," J.Aircraft, Vol 115, No 7: 399-406 (Jul 1978).

15. Cole,J.D. Perturbation Methods in Applied Mechanics. Preface. Waltham, Massachusets: Blaisdell Pub. Co. 1968.

16. Jameson,A. "Transonic Flow Calculations for Airfoils and Bodies of Revolution," Grumman Aerospace Corporation Aerodynamics Report 390-71-1.

17. Winz,H.J. and Smolderer,J.J. Numerical Methods in Fluid Dynamics. 2-4, 30-33. Washington, D.C.: Hemisphere Publishing Co. 1978.

18. Chin,W.C. "Goethert's Rule with an Improved Boundary Condition," AIAA Journal, Vol 15, No 10: 1516-1518. (Oct 1977).

19. Van Dyke,M. Perturbation Methods in Fluid Mechanics. Stanford, California: The Parabolic Press. 1975.

20. Hayes,W.D. "Second-Order Pressure Law for Two-Dimensional Compressible Flow," J.Aero.Sci., 22: 284-286 (Apr 1955)

21. Clancy,L.J. Aerodynamics. 325-330. New York: John Wiley and Sons, 1975.

22. Kaplun,S. Fluid Mechanics and Singular Perturbations. New York: Academic Press, 1967.

23. Schneider,W. "A Note on a Breakdown of the Multiplicative Composition of Inner and Outer Expansions," J.Fluid Mech., Vol 59, Part 4: 785-789 (1973).

24. Abbott,I.H. and Von Doenhoff,A.E. Theory of Wing Sections. New York: Dover Publications, Inc., 1959.

25. Emmons,H.W. "Flow of a Compressible Fluid Past a Symmetrical Airfoil in a Wind Tunnel and in Free Air," NACA TN 1746. 1948.

26. Amick,J.L. "Comparison of the Experimental Pressure Distribution on as NACA 0012 Profile at High Speeds with that Calculated by the Relaxation Method," NACA TN 2174, 1950.

27. Jonas,F.M. "Subsonic Aerodynamic Characteristics of Proposed High Wing Maneuvering Air-to-Surface Submunitions," USAFA TR-76-13, AFATL TR-76-58. 1976.

28. Kellogg,O.D. Foundations of Potential Theory. 216-218. New York: Dover Publications, Inc., 1953.

Appendix A: First Order Analytic Solution for an Elliptic Cylinder in Subsonic Flow

As presented in Chapter III, Eqs (III-2) through (III-5), the outer, inner, and intermediate first order problems for the elliptic cylinder (Fig 2), whose surface is given by

$$F(x,z) = x^2 + \left(\frac{z}{c}\right)^2 - 1 = 0 \qquad \text{(A-1)}$$

in the subsonic compressible isentropic flow of a perfect gas (γ=1.4) are all of the form

$$B^2\varphi_{1xx} + \varphi_{1zz} = 0 \qquad \text{(A-2)}$$

$$\left\{\left[\left(1-\frac{A}{2}\right)B^2\right] + \tau B^2\varphi_{1x}\right\}x + \tau\varphi_{1z}\left(\frac{z}{c^2}\right) = 0 \text{ on } F(x,z)=0 \qquad \text{(A-3)}$$

$$\varphi_{1x} \to A/2\tau\,,\ \varphi_{1z} \to 0 \quad \text{at infinity} \qquad \text{(A-4)}$$

where

$$B^2 = \begin{cases} \beta^2, \text{ outer } (A=0),\ \tau = \epsilon \\ \Delta, \text{ intermediate } (0<A<2),\ \tau = \epsilon\epsilon^{A/2} \\ 1, \text{ inner } (A=2),\ \tau = \epsilon^2 \end{cases} \qquad \text{(A-5)}$$

To transform the problem to the incompressible flow case about an equivalent elliptic cylinder let $\bar{x} = x/B$, $\bar{\varphi} = B\tau\varphi$ (where $B\neq 0$), and $\Phi = \left(1-\frac{A}{2}B^2\right)\bar{x} + \bar{\varphi}$ resulting in

$$\Phi_{1\bar{x}\bar{x}} + \Phi_{1zz} = 0 \qquad \text{(A-6)}$$

$$\Phi_{1\bar{x}}(B^2\bar{x}) + \Phi_{1z}\left(\frac{z}{c^2}\right) = 0 \quad \text{on } F(\bar{x},z)=0 \qquad \text{(A-7)}$$

$$\Phi_{1\bar{x}} \to 1,\ \Phi_{1z} \to 0 \quad \text{at infinity} \qquad \text{(A-8)}$$

The problem is now mapped to a known solution, the circular cylinder in incompressible flow, using the Joukowski transform and its inverse. First, however, it is necessary to determine the Joukowski transform constants when mapping from the circle to the ellipse where

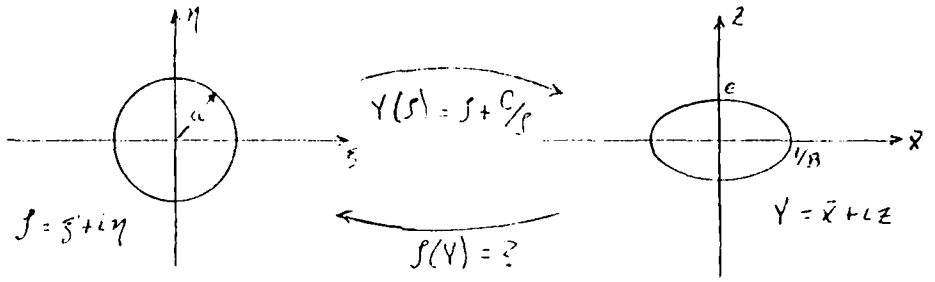

The known solution, represented by the complex potential, in the ξ-η plane is

$$\mathcal{F}(f) = \Phi(f) + i\psi(f)$$
$$= f + a^2/f \qquad \text{(A-9)}$$

The circle radius, a, and the constant C in the Joukowski transform are determined to be

$$a = \frac{1}{2B}(1 + B\epsilon) \qquad \text{(A-10)}$$

$$C = \frac{1}{4B^2}(1 - B^2\epsilon^2) \qquad \text{(A-11)}$$

Next, the inverse transform is determined to be

$$f(Y) = \frac{1}{2}\left(Y + \sqrt{Y^2 - 4C}\right) \qquad \text{(A-12)}$$

It becomes necessary at this point to introduce elliptic coordinates so that the inverse transform and resulting complex potential may be separated into distinct real and imaginary parts (this cannot be done in Eq (A-12)). Let

$$Y = k\,ch\,\gamma, \quad \bar{Y} = k\,ch\,\bar{\gamma} \qquad \text{(A-13)}$$

where

$$\gamma = \mu + i\nu, \quad \bar{\gamma} = \mu - i\nu \qquad \text{(A-14)}$$

resulting in

$$\bar{X} = k\,ch\mu\cos\nu \quad \text{where } ch \triangleq \cosh \qquad \text{(A-15)}$$

$$Z = k\,sh\mu\sin\nu \quad \text{where } sh \triangleq \sinh \qquad \text{(A-16)}$$

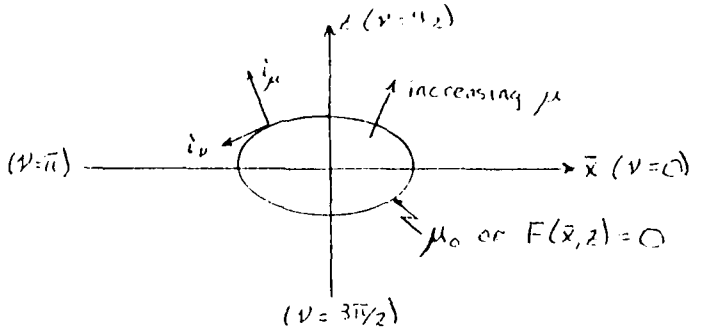

$$0 \le \nu < 2\pi \,, \quad \mu_o \le \mu \tag{A-17}$$

It is interesting to note that in elliptic coordinates the surface boundary condition is simply

$$\Phi_{,\mu}\big|_{\mu_o} = 0 \tag{A-18}$$

where the total velocity is given by

$$\vec{V} = \frac{1}{k\sqrt{\cosh^2\mu - \cos^2\nu}} \left\{ \Phi_{,\mu}\, i_\mu + \Phi_{,\nu}\, i_\nu \right\} \tag{A-19}$$

Since

$$\cos^2\nu + \sinh^2\nu = 1 = \left(\frac{\bar{x}}{k\cosh\mu}\right)^2 + \left(\frac{z}{k\sinh\mu}\right)^2 \tag{A-20}$$

and the surface of the ellipse is given by

$$(B\bar{x})^2 + (z/\epsilon)^2 = 1$$

then

$$\cosh\mu_o = 1/Bk \,, \quad \sinh\mu_o = \epsilon/k \tag{A-21}$$

or

$$\mu_o = \ln\sqrt{\frac{1+BC}{1-BC}} \tag{A-22}$$

specifying the surface F(x̄,z)=0. From

$$\cosh^2\mu_o - \sinh^2\mu_o = 1 \tag{A-23}$$

we find

$$k = \frac{1}{B}\sqrt{1-(BC)^2} = \sqrt{4C^2} \tag{A-24}$$

From

$$\mu + i\nu = \cosh^{-1}\left[\frac{1}{k}(\bar{x} + iz)\right] \tag{A-25}$$

we find

$$\mu = \cosh^{-1}(P+q/2k) \tag{A-26}$$

$$\nu = \cos^{-1}(P-q/2k) \tag{A-27}$$

where

$$P = \sqrt{z^2+(x+L)^2} \tag{A-28}$$

$$q = \sqrt{z^2+(x-L)^2} \tag{A-29}$$

Finally, the inverse transform is given by

$$f(\gamma_0) = \frac{k}{2} e^{\gamma} \tag{A-30}$$

The potential is then given by

$$\Phi_1(\mu,\nu) = \frac{k}{2}\left\{e^{\mu} + \left(\frac{1+B\epsilon}{1-B\epsilon}\right)e^{-\mu}\right\}\cos\nu + \text{constant} \tag{A-31}$$

Note, the arbitrary constant in Eq (A-31) results since this is a Neumann problem. Returning to the (x,z) coordinates, the first order analytic solution for an elliptic cylinder is given by

$$\Phi_1(x,z) = \frac{kQ}{2B\epsilon}\left\{\left(Q+\sqrt{Q^2-1}\right)\left\{1+R^2\right\} - \left(1-\frac{AB^2}{2}\right)\frac{x}{\epsilon B^2}\right\} + \text{constant} \tag{A-32}$$

where

$$P = P+q/2k \tag{A-33}$$

$$Q = P-q/2k \tag{A-34}$$

$$R = \sqrt{\frac{1+B\epsilon}{1-B\epsilon}}\Big/\left(Q+\sqrt{Q^2-1}\right) \tag{A-35}$$

Appendix B: Thin Airfoil Theory Solution for an Elliptic Cylinder in Subsonic Flow

The equations for the flow over an elliptic cylinder (Fig 2) in incompressible flow given by thin airfoil theory are:

$$\varphi_{xx} + \varphi_{zz} = 0 \tag{B-1}$$

$$\varphi_z(x,0^{\pm}) = \left.\frac{dz_t}{dx}\right|_{u,l} \text{ on } z_t = \pm c\sqrt{1-x^2},\ |x| \le 1 \tag{B-2}$$

$$|\nabla\varphi| \to 0 \text{ at infinity} \tag{B-3}$$

Assuming the solution can be given by the following expression,

$$\varphi(x,z) = \frac{1}{4\pi}\int_{-1}^{1} Q(\xi,0)\ln\sqrt{(x-\xi)^2+z^2}\,d\xi \tag{B-4}$$

which represents a source distribution on the x-axis, $|x| \le 1$, where $Q(\xi,0)$ is the source strength. The perturbation components of velocity are given by:

$$\varphi_x = \frac{u}{U_\infty} = \frac{1}{2\pi}\int_{-1}^{1} \frac{Q(\xi,0)(x-\xi)}{(x-\xi)^2+z^2}\,d\xi \tag{B-5}$$

$$\varphi_z = \frac{w}{U_\infty} = \frac{1}{2\pi}\int_{-1}^{1} \frac{z\,Q(\xi,0)}{(x-\xi)^2+z^2}\,d\xi \tag{B-6}$$

To first order from conservation of mass the source strength is given by:

$$Q(x,0) \cong 2\frac{dz_t}{dx} \tag{B-7}$$

The surface perturbation velocity is thus given by,

$$\begin{aligned}\varphi_x(x,0^{\pm}) &\cong \frac{1}{2\pi}\oint_{-1}^{1}\frac{Q(\xi,0)}{(x-\xi)}\,d\xi = \frac{1}{2\pi}\oint_{-1}^{1}\frac{\left.\frac{dz_t}{dx}\right|_{x=\xi}}{(x-\xi)}\,d\xi \\ &\cong \frac{1}{\pi}\oint_{-1}^{1}\frac{(-c)\,\xi\,d\xi}{(x-\xi)\sqrt{1-\xi^2}}, \\ &= C \quad \text{for } x^2 < 1\end{aligned} \tag{B-8}$$

with the surface velocity being:

$$\frac{V}{U_\infty} = 1 + C \tag{B-9}$$

Applying the Prandtl-Glauert compressibility correction gives

the following subsonic surface velocity:

$$\frac{V}{U_\infty} = 1 + 1/\sqrt{1 - M_\infty^2} \qquad \text{(B-10)}$$

It is quickly noted that this value is constant for a given free stream Mach number, M_∞.

AD-A096 057 AIR FORCE INST OF TECH WRIGHT-PATTERSON AFB OH SCHOO--ETC F/G 20/4
A SINGULAR PERTURBATION METHOD FOR ARBITRARY CONFIGURATIONS IN --ETC(U)
OCT 80 F M JONAS
UNCLASSIFIED AFIT/DS/AA/80-3 NL

2 OF 2
AD A096057

END
DATE FILMED
4-81
DTIC

Appendix C: Thin Airfoil Theory Solution for a NACA 0012 Airfoil in Subsonic Flow

Following the procedure of Appendix B, the surface perturbation velocity in incompressible flow is given by:

$$\varphi_x(x,0^{\pm}) = \frac{u}{U_\infty} = \frac{1}{2\pi}\int_{-1}^{1}\frac{\Delta(\xi,0)}{(x-\xi)}\,d\xi = \frac{1}{\pi}\int\frac{\left.\frac{dz_t}{dx}\right|_{x=\xi}}{(x-\xi)}\,d\xi \qquad \text{(C-1)}$$

The surface of the airfoil (Fig 9) is described by,

$$z_t = \pm\left\{.252\sqrt{x+1} - .146 - .189x - .023x^2 + .012x^3 - .008x^4\right\} \qquad \text{(C-2)}$$

where $|x| \leq 1$. Applying the surface boundary condition, Eq (B-7), results in:

$$\frac{u}{U_\infty} = \frac{1}{\pi}\int_{-1}^{1}\left\{(.176)\left(\frac{1}{\sqrt{\xi+1}(x-\xi)}\right) - \frac{.189}{(x-\xi)} - \frac{.046\,\xi}{(x-\xi)} + \frac{.036\,\xi^2}{(x-\xi)} - \frac{.032\,\xi^3}{(x-\xi)}\right\}d\xi$$

$$= \frac{1}{\pi}\left\{(.176)\frac{1}{\sqrt{1+x}}\ln\frac{\sqrt{2}+\sqrt{1+x}}{\sqrt{2}-\sqrt{1+x}} - (.189)\ln\frac{1+x}{1-x} + \left(x\ln\frac{1+x}{1-x}-2\right)\left(-.046+.036x-.032x^2\right) + \left(\frac{\xi}{3}\right)(.008)\right\} \qquad \text{(C-3)}$$

The resulting surface velocity is,

$$\frac{V}{U_\infty} = 1 + \frac{u}{U_\infty} \qquad \text{(C-4)}$$

with the result for compressible flow being given by:

$$\frac{V}{U_\infty} = 1 + \left.\frac{u}{U_\infty}\right|_{M=0} \Big/ \sqrt{1-M_\infty^2} \qquad \text{(C-5)}$$

This expression for the surface velocity results in infinite or undefined velocities at the leading and trailing edges of the given airfoil.

Appendix D: Second Order Analytic Solution for an Elliptic Cylinder in Subsonic Flow

For application of the second order method, consider the nonlifting elliptic cylinder (Fig 2) in the subsonic compressible isentropic flow of a perfect gas (γ=1.4). The surface of the ellipse is given by Eq (III-1). The second order outer (A=0), intermediate (0<A<2), and inner problems are of the form

$$B^2\phi_{xx}+\phi_{zz}=M^2\lambda\phi_x\phi_{xx}+2M^2\phi_z\phi_{xz} \qquad \text{(D-1)}$$

$$(B^2\phi_x)x+\phi_z\left(\frac{\partial z}{\partial z}\right)=0 \quad \text{on } F(x,z)=0 \qquad \text{(D-2)}$$

$$|\nabla\phi|\to 0 \quad \text{at infinity} \qquad \text{(D-3)}$$

where

$$M^2=\begin{cases} M_\infty^2, & \text{outer } (A=0) \\ \Delta_1, & \text{intermediate } (0<A<2) \\ 0, & \text{inner } (A=2) \end{cases} \qquad \text{(D-4)}$$

$$\lambda=(\gamma+1)-(\gamma-1)B^2 \qquad \text{(D-5)}$$

It can be shown that the solution to this problem, if it exists, is unique to within an unknown constant (e.g., let ψ_1 and ψ_2 be two solutions then ψ, where $\psi=\psi_1-\psi_2$, is equal to a constant). From the Divergence Theorem for infinite domains (Ref 28) one can also show the following compatibility condition must be satisfied for a solution to exist (the domain ν representing the region from the surface of the ellipse to some circular boundary at infinity):

$$\int_\nu\left(M^2\lambda\phi_x\phi_{xx}+2M^2\phi_z\phi_{xz}\right)d\nu=0 \qquad \text{(D-6)}$$

It is quickly noted that this condition is satisfied for a free stream Mach number of zero, or incompressible flow.

This is indeed true for the inner approximation where the solution can easily be shown to be

$$\varphi_2^i(x,z) = \text{constant} \tag{D-7}$$

and thus

$$\varphi_{2x}^i = \varphi_{2z}^i = 0 \tag{D-8}$$

Equation (D-6) represents a necessary and sufficient condition for the existance of second order solutions. For compressible flow Eqn (D-6) can be shown to be satisfied for the elliptic cylinder and thus we are assured of the existence of an analytic solution for the second order outer and intermediate problems and a second order composite solution. This in turn reinforces the credibility of the first order method as will also be demonstrated in Appendix E. Given the demonstrated accuracy of the first order method however, plus the ease of obtaining first order solutions as compared to a second order effort, the first order method should be sufficient for most applications.

Appendix E: Surface Values of $\beta^2\varphi_{xx}+\varphi_{zz}$ for the 2-D Ellipse in Subsonic Flow

In this Appendix some interesting comparisons of the surface values of the term $\beta^2\varphi_{xx}+\varphi_{zz}$ as evaluated exactly (numerically) and by various approximations are shown in Figs E1a-f (the legend for these Figs is in Table IV). The exact value of $\beta^2\varphi_{xx}+\varphi_{zz}$, obtained numerically using results from the Jameson code, represents the exact perturbation potential equation, Eq (II-9). The approximations are developed using the first order results with $\varphi_1^c(x,z)$ being formed using the additive composition, or,

$$\varphi_1^c(x,z) = \varphi_1^o(x,z) + \varphi_1^i(x,z) - \varphi_1^I(x,z) \qquad \text{(E-1)}$$

Note that this assumed composite solution is not the same as the composite solutions used previously for the velocity (Eqs (II-39), (II-40)), although the form is the same. Analytic results, representing various approximations, are shown for the first order outer or Prandtl-Glauert equation,

$$\beta^2\varphi_{1xx}^o + \varphi_{1zz}^o = 0 \qquad \text{(E-2)}$$

the first order additive composite (A=1)

$$\begin{aligned}\beta^2\varphi_{1xx}^c + \varphi_{1zz}^c &= \beta^2\left[\varphi_{1xx}^o+\varphi_{1xx}^i-\varphi_{1xx}^I\right] + \left[\varphi_{1zz}^o+\varphi_{1zz}^i-\varphi_{1zz}^I\right] \\ &= \beta^2\left[\varphi_{1xx}^i-\varphi_{1xx}^I\right] + \left[\varphi_{1zz}^i-\varphi_{1zz}^I\right] \qquad \text{(E-3)}\end{aligned}$$

and the second order additive composite (A=1) using the first order solutions

$$\begin{aligned}\beta^2\varphi_{2xx}^c + \varphi_{2zz}^c = {} & M_\infty^2\left[(\gamma+1)-(\gamma-1)\beta^2\right]\varphi_{1xx}^c\varphi_{1x}^c \\ & + 2M_\infty^2\varphi_{1x}^c\varphi_{1xz}^c \qquad \text{(E-4)}\end{aligned}$$

As seen in Figs E1a-f the Prandtl-Glauert equation is of course equal to zero for all Mach numbers, but it (as well as

Table IV

Legend for Figures E1a-f

2-D Ellipse

o Jameson, $\beta^2\varphi_{xx} + \varphi_{zz}$

—— 1st Order Additive Composite (A=1), $\beta^2\varphi^c_{1xx} + \varphi^c_{1zz}$

—·— 1st Order Additive Composite (A=1), Approximation to 2nd Order Equation, $\beta^2\varphi^c_{2xx} + \varphi^c_{2zz}$

---- 1st Order Outer Equation $\beta^2\varphi^o_{1xx} + \varphi^o_{1zz} = 0$

the other approximations) is an excellent approximation compared to the exact solution to the flow over the majority of the body where the assumption of small perturbations is valid. The exception to this occurs in or near the stagnation region, and, as represented by the exact solution, the flowfield is seen to be distinctly divided into two regions. The first and second order approximations more closely approximate the exact solution (especially in the stagnation region), with the second order approximation being almost identical to the exact solution for all Mach numbers except at M_∞=0.8 (transonic flow). The change in character of the exact solution as one approaches the transonic flow regime (M_∞=0.8) clearly shows another approach is required to obtain more accurate results in this flow regime. To conclude however, these comparisons once again demonstrate that the method as developed yields solutions that are uniformly valid, however it is applied.

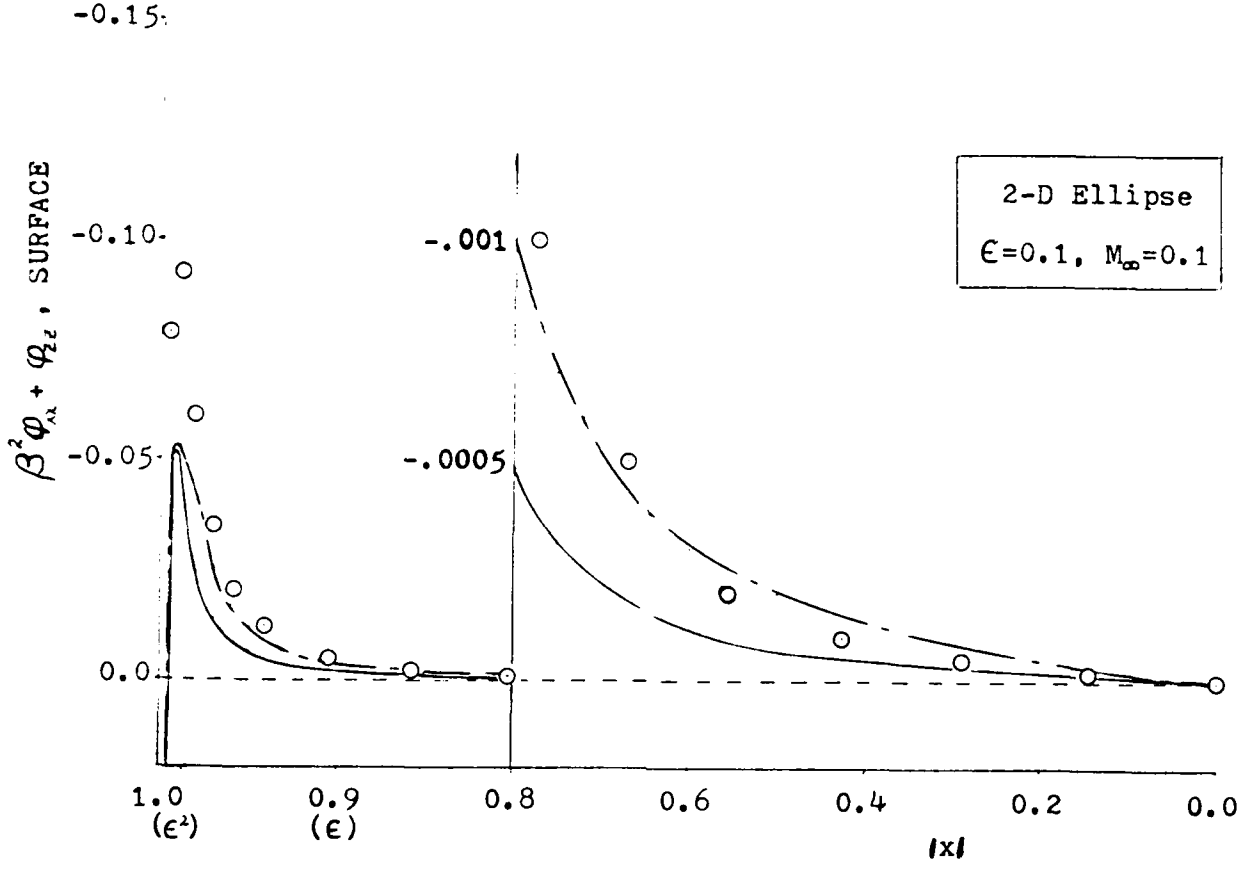

Figure E1a. Comparison of Surface Values, $\beta^2\varphi_{xx}+\varphi_{zz}$, Jameson, First Order Outer (Thin Airfoil Theory), First Order Additive (A=1) Composite, and First Order Additive (A=1) Composite Approximation of the Second Order Equation, 2-D Ellipse, 0-50% Chord, ϵ=0.1, M_∞=0.1

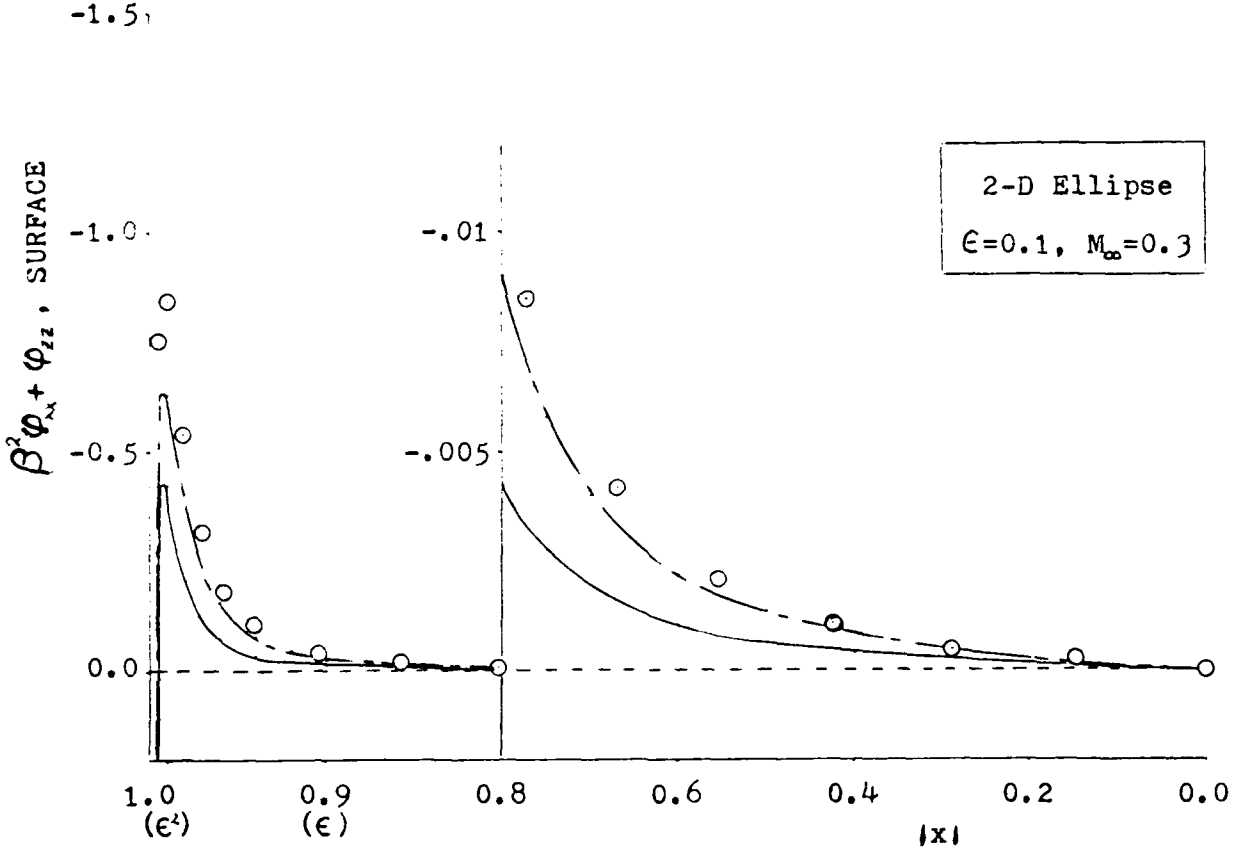

Figure E1b. (continued), ϵ=0.1, M_∞=0.3

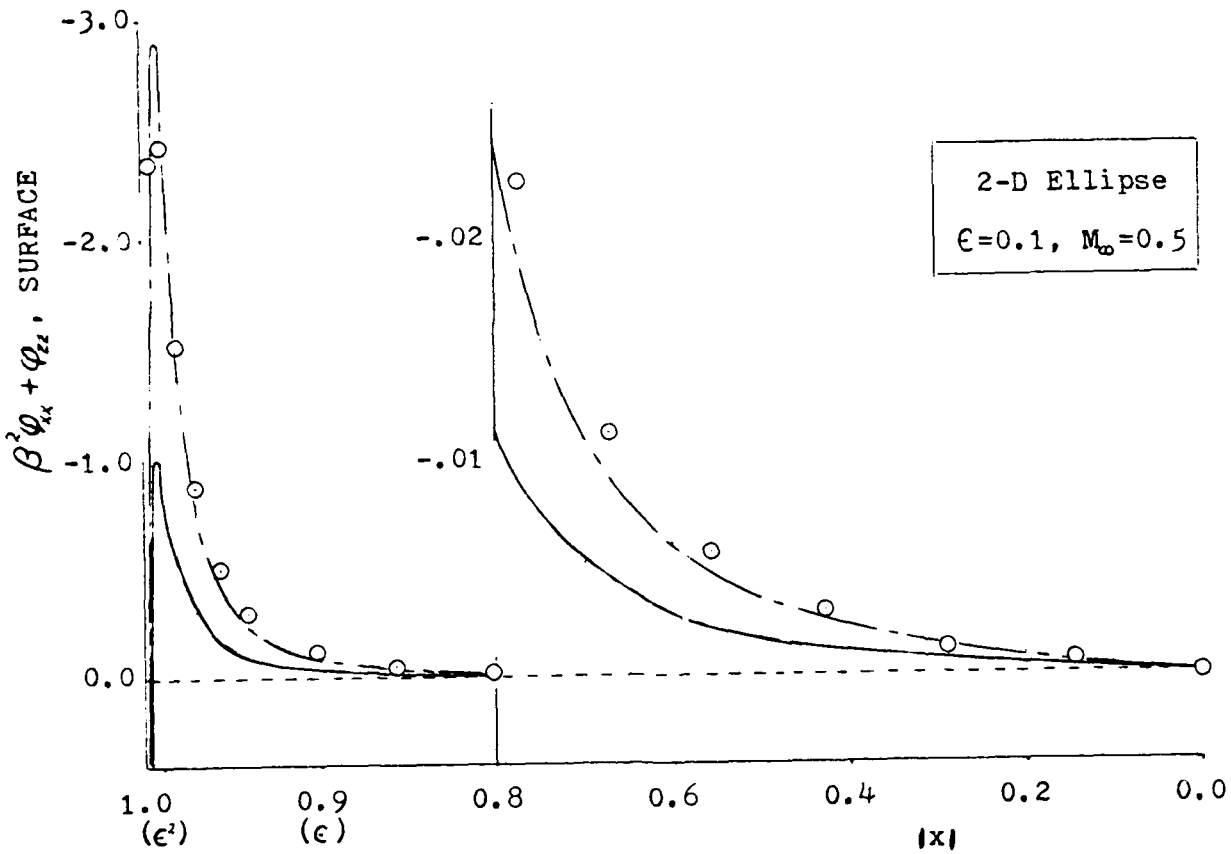

Figure E1c. (continued), ϵ=0.1, M_∞=0.5

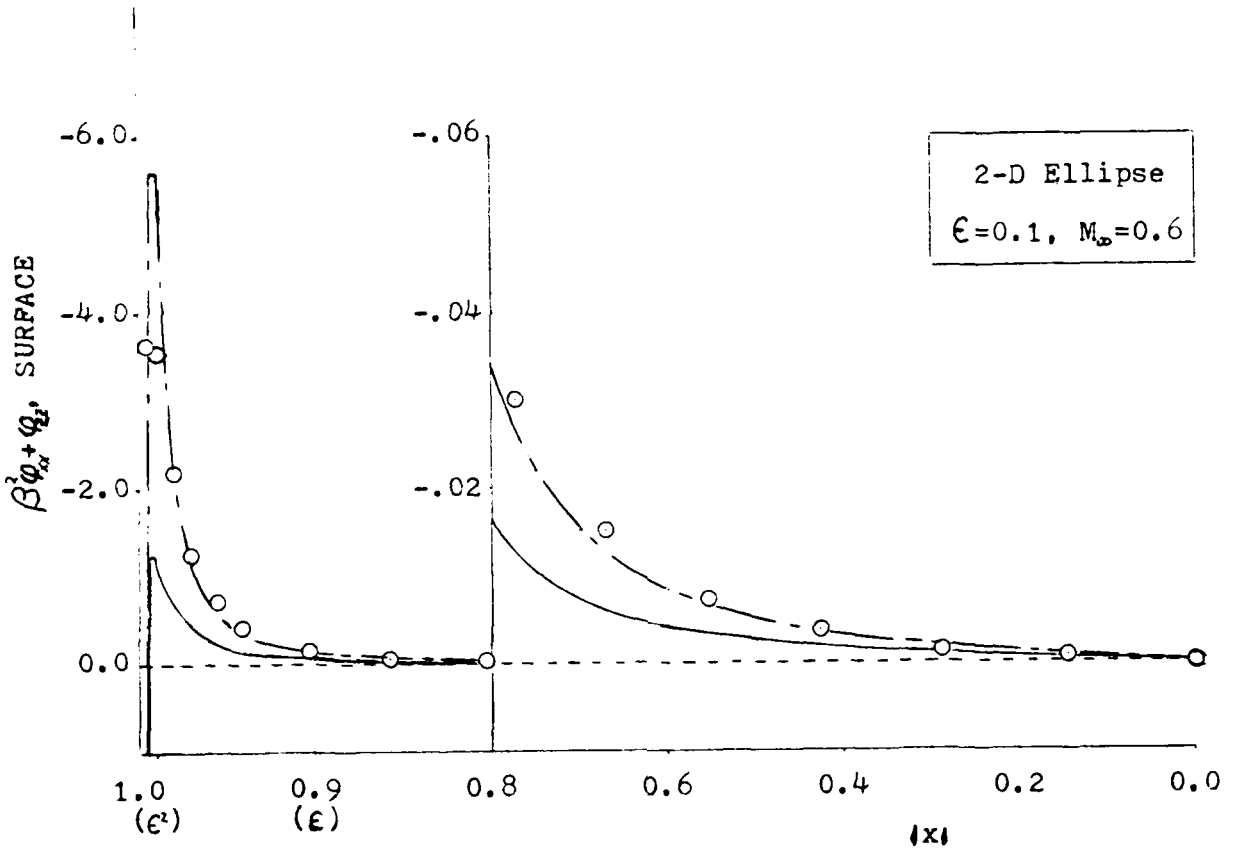

Figure E1d. (continued), ϵ=0.1, M_∞=0.6

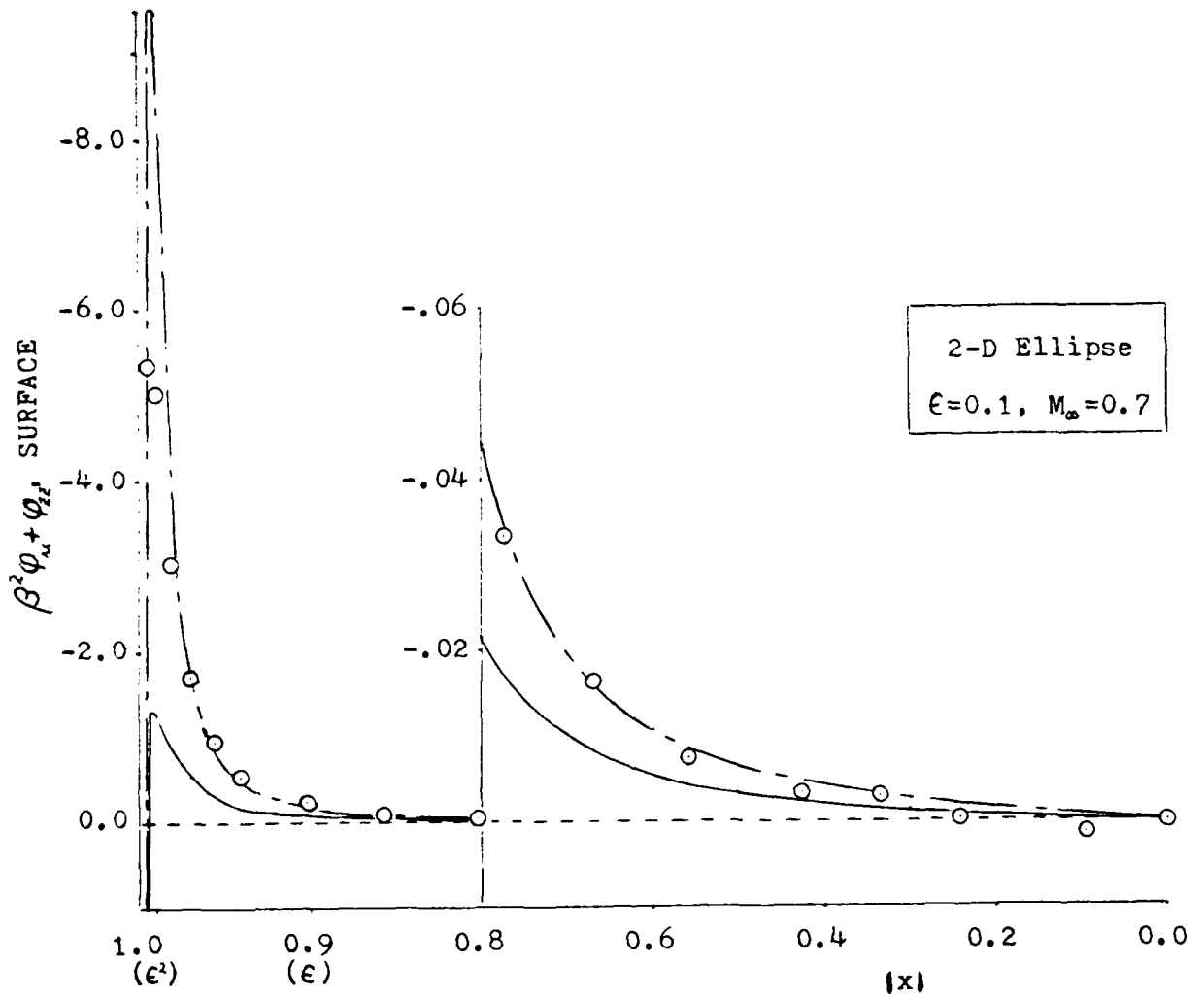

Figure E1e. (continued), ϵ=0.1, M_∞=0.7

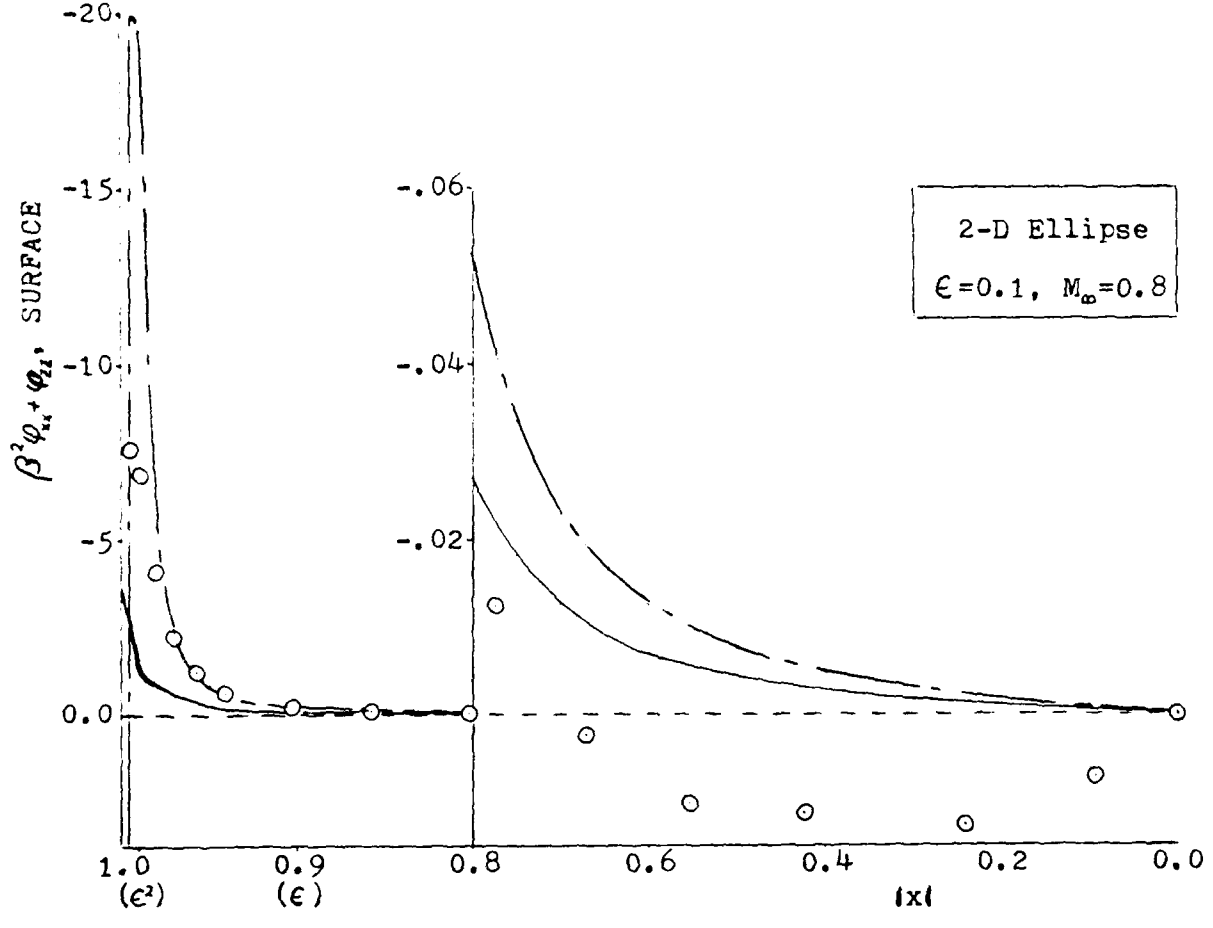

Figure E1f. (continued), ϵ=0.1, M_∞=0.8

VITA

Frederick Morgan Jonas was born 18 February 1948, in Gallup, New Mexico where he graduated from high school in 1966. He attended the United States Air Force Academy from which he received a Bachelor of Science in Aeronautical Engineering degree in June 1970. Entering the United States Air Force immediately upon graduation he then attended The Leland Stanford Junior University through the Air Force Institute of Technology where he received the degree of Master of Science in June 1971, studying in aeronautical and astronautical engineering. He then served at the Arnold Engineering Development Center, Directorate of Test, Arnold AFS, Tennessee, from June 1971 through June 1974. Next he served as an instructor at the United States Air Force Academy, Department of Aeronautics from July 1974 through July 1976. He then entered the School of Engineering, Air Force Institute of Technology, in September 1976.

Unclassified

SECURITY CLASSIFICATION OF THIS PAGE (When Data Entered)

REPORT DOCUMENTATION PAGE		READ INSTRUCTIONS BEFORE COMPLETING FORM
1. REPORT NUMBER AFIT/DS/AA/80-3	2. GOVT ACCESSION NO. AD-A096 651	3. RECIPIENT'S CATALOG NUMBER
4. TITLE (and Subtitle) A SINGULAR PERTURBATION METHOD FOR ARBITRARY CONFIGURATIONS IN SUBSONIC POTENTIAL FLOW		5. TYPE OF REPORT & PERIOD COVERED Dissertation (PhD) 6. PERFORMING ORG. REPORT NUMBER
7. AUTHOR(s) Frederick M. Jonas, Capt, USAF		8. CONTRACT OR GRANT NUMBER(s)
9. PERFORMING ORGANIZATION NAME AND ADDRESS Air Force Institute of Technology AFIT/EN Wright-Patterson AFB, Ohio 45433		10. PROGRAM ELEMENT, PROJECT, TASK AREA & WORK UNIT NUMBERS
11. CONTROLLING OFFICE NAME AND ADDRESS		12. REPORT DATE October 1980 13. NUMBER OF PAGES 105
14. MONITORING AGENCY NAME & ADDRESS(if different from Controlling Office)		15. SECURITY CLASS. (of this report) Unclassified 15a. DECLASSIFICATION DOWNGRADING SCHEDULE

16. DISTRIBUTION STATEMENT (of this Report)

Approved for public release; distribution unlimited

17. DISTRIBUTION STATEMENT (of the abstract entered in Block 20, if different from Report)

FREDRIC C. LYNCH, Major, USAF
Director of Public Affairs
17 FEB 1981

18. SUPPLEMENTARY NOTES

Air Force Institute of Technology (ATC)
Wright-Patterson AFB, OH 45433

19. KEY WORDS (Continue on reverse side if necessary and identify by block number)

Perturbation method	Composite Solution
Potential Flow	Prandtl-Glauert Equation
Inviscid	2-D/3-D Flow
Expansions	Drag
Stagnation Region	

20. ABSTRACT (Continue on reverse side if necessary and identify by block number)

A method is developed for obtaining uniformly valid solutions about slender bodies (2-D or 3-D) with round leading/trailing edges in compressible subsonic flow. The method is based on the principles of singular perturbation theory and applied to nonlifting thickness problems. The method corrects small perturbation theory (outer solution) with a stagnation region theory (inner solution) yielding uniformly

DD FORM 1 JAN 73 1473 EDITION OF 1 NOV 65 IS OBSOLETE

Unclassified

SECURITY CLASSIFICATION OF THIS PAGE (When Data Entered)

20. (continued)

valid solutions. Analytic results of the first and second order method are presented and compared to other methods, including exact numerical results, for the elliptic cylinder. The first order method is shown to be preferred to higher order efforts and is directly applicable to current numerical techniques solving the Prandtl-Glauert equation. Application of the first order method numerically, using a current panel technique, is presented for the NACA 0012 airfoil and a glide bomb configuration. All comparisons of the first order composite results with other methods show excellent agreement and improved results subject to the limits of validity of the theory. The ability to correctly model the flow behavior in stagnation regions using the composite solutions leads to a greater confidence in aerodynamic predictions, especially inviscid drag estimates.